International Journal of Bifurcation and Chaos, Vol. 12, No. 3 (2002) 535–559

NONISOTROPIC SPATIOTEMPORAL CHAOTIC VIBRATION OF THE WAVE EQUATION DUE TO MIXING ENERGY TRANSPORT AND A VAN DER POL BOUNDARY CONDITION

GOONG CHEN*
Department of Mathematics, Texas A&M University, College Station, TX 77843, USA
SZE-BI HSU
Department of Mathematics, Tsing Hua University, Hsinchu, Taiwan, R.O.C.
JIANXIN ZHOU†
Department of Mathematics, Texas A&M University, College Station, TX 77843, USA

Received April 26, 2001; Revised June 5, 2001

The *imbalance* of the boundary energy flow due to energy injection at one end and a nonlinear van der Pol boundary condition at the other end of the spatial one-dimensional interval can cause chaotic vibration of the linear wave equation [Chen *et al.*, 1998b, 1998c]. However, such chaotic vibration is *isotropic* with respect to space and time because the two associated families of characteristics both propagate with the same speed and, thus, the "strength of chaos" is the same along both x and t directions. In this paper, we show that by including a mixed partial derivative linear energy transport term in the wave equation, nonlinearity in the van der Pol boundary condition can also cause chaotic vibration (without energy injection from the other end). Two new families of characteristics now travel with different speeds, leading to strong mixing of waves and *nonisotropic spatiotemporal chaos*. Parameter range for the route to chaos, including period-doubling, homoclinic orbits and Cantor-like invariant sets is classified. Numerical simulations of chaotic space-time profiles are also illustrated.

Keywords: Nonisotropic spatiotemporal chaos; wave equation; van der Pol boundary condition.

1. Introduction and Model Formulation

Earlier, in a series of papers [Chen *et al.*, 1998a–1998d], we studied nonlinear vibration of the one-dimensional (1D) wave equation on a bounded interval with a van der Pol boundary condition. Chaos occurs, for example, when there is energy injection either from the other end of the interval [Chen *et al.*, 1998b] or at the middle-of-the-span point [Chen *et al.*, 1998d]. Related studies have been done in [Sharkovsky *et al.*, 1993, 1994] and [Shimura *et al.*, 1967], for example. A major reason that has motivated us to study such problems is that the 1D wave equation is a rather *basic* distributed parameter model for mechanical vibration, such as vibrating strings and acoustic wave propagation. With given or designed nonlinear boundary conditions/controllers,

*Work completed while visiting the National Center for Theoretical Science, Tsing Hua University, Hsinchu, Taiwan, R.O.C. Supported in part by NSF Grant DMS 96-10076, Texas ARP Grant 010366-046, and Texas A&M University Interdisciplinary Research Initiative 96-36 and 99-22.
†Supported in part by a grant from the National Council of Science of R.O.C.

the solution is amenable to a thoroughly rigorous mathematical analysis, revealing immensely rich dynamical behavior suitable for possible future technological applications. On the one hand, we have tried to explore the useful, *microscosmic* nature of spatiotemporal chaos in 1D wave propagation, in particular, in *acoustics*; on the other hand, the knowledge gained will improve our understanding of *macrocosmic chaos* in complex, general distributed parameter systems, which will be the ultimate objective for investigation.

Elsewhere, in engineering, as far as acoustic chaos is concerned, there has been a sharp surge of interest in recent years. A good number of papers [Herzel, 1993; Holzfuss & Lauterborn, 1989; Idogawa *et al.*, 1993; Katz, 1996; Lauterborn *et al.*, 1996; Lauterborn & Cramer, 1981; Lauterborn & Holzfuss, 1986; Mcintyre *et al.*, 1983; Mende *et al.*, 1990; Shigesada *et al.*, 1979; Smith *et al.*, 1982; Stinecke & Herzel, 1995; Swift, 1988, 1995; Tufilaro, 1989; Yazaki, 1993], have been published. We may mention, for example, the following research and applications:

(i) In [Lauterborn *et al.*, 1996], the collaborative German and Russian scientists studied chaotic motions in acoustic cavitation, which understandably is important for the detection of a submarine's underwater acoustic signature;
(ii) the development of musical instruments that play new types of sounds generated by chaotic acoustics, along with the corresponding musical notes to be composed by musicians [Idogawa *et al.*, 1993; Swift, 1988, 1995];
(iii) study of sounds made by the vocal cords in the speech production process has revealed bifurcation and chaotic dynamics that could be used for personal (voice) identification and health diagnosis (for newborn infants from their cries [Mende *et al.*, 1990]);
(iv) the design of *thermoacoustic* oscillators as possible musical instruments playing both ordinary and chaotic musical notes, and cooling/heating *thermoacoustic engines* whose control is achieved by boundary heating/cooling [Swift, 1988, 1995].

Most of the above-mentioned references emphasize experimental and/or modeling work with real-world applications, but did not provide rigorous mathematical analysis. Nevertheless, some of their physical motivations are quite inspiring; see the discussion below.

Return to our work [Chen *et al.*, 1998a–1998d]. The study of the chaotic vibration of the 1D wave equation therein, although *spatiotemporal* in nature, is essentially *isotropic with respect to space and time*. There are at least two reasons for this: first, the wave equation $w_{xx} - w_{tt} = 0$ is invariant under the changes of variables

$$(x, t) \to (-x, t),\ (x, t) \to (x, -t),\ (x, t) \to (t, x) \tag{1}$$

and, thus, the symmetry structure between x and $\pm t$ of the equation itself is extremely strong. (Indeed, if there were no boundary conditions, then x and $\pm t$ may be regarded as "identical".) Second, the two families of characteristics belong to the wave equation both travel with the same speed, again making x and $\pm t$ indiscernible and, thus, we may say that "the strength of chaos" is the same in both the x and t directions. The spatiotemporal-isotropic nature of the solutions studied in [Chen *et al.*, 1998a–1998d] is evident in explicit representations like [Chen *et al.*, 1998b, p. 425, (13), (14)], and in the many graphics of solution profiles displayed in [Chen *et al.*, 1998b, 1998c]. For an immediate comparison, see the graphics in Sec. 6 below.

Obviously, for nonisotropic spatiotemporal chaos to happen, a key element is to have a medium which is not spatially homogeneous. Thus, for the wave equation, we need something else in the equation that is *not invariant* with respect to the change of variables (1). One might attempt to add a variable coefficient term (say, $a(x)w(x, t)$) to the wave equation. However, this makes the mathematical treatment rather difficult. Here we have found a sufficiently simple medium in which waves traveling to the left and the right have different speeds. The model equation in this paper is the following hyperbolic equation

$$w_{xx}(x, t) - \nu w_{xt}(x, t) - w_{tt}(x, t) = 0\,, \qquad 0 < x < 1\,, \quad t > 0\,, \tag{2}$$

where ν is a positive constant and where, for the mere sake of convenience, we have set the coefficient for the $-w_{tt}$ term in (7) to be 1 as well, because the mathematical analysis in this paper goes through with only straightforward modifications as long as $-w_{tt}$ is multiplied by a positive constant. Equation (2) differs from the standard wave equation $w_{xx} - w_{tt} = 0$ by the presence of the "mixed term" $-\nu w_{xt}$. Let us now make precise the physical

origin of this term. Consider acoustic waves traveling in a pipe filled with a gas moving with speed $c : 0 < c < 1$ to the left, such as air blown into a clarinet in the aforementioned papers [Idogawa *et al.*, 1993; Swift, 1988, 1995] on chaotic musical instruments. Assume that an observer travels with the gas, measures the acoustic pressure field and finds that it satisfies the wave equation

$$\frac{\partial^2 w(x,\,t)}{\partial x^2} - \frac{\partial^2 w(x,\,t)}{\partial t^2} = 0\,. \tag{3}$$

A *stationary* observer is also making measurements of the same acoustic wave propagation. His coordinate system is therefore

$$x' = x + ct\,, \quad t' = t\,. \tag{4}$$

He will find that the equation for the acoustic pressure field is necessarily

$$(1-c^2)\frac{\partial^2 w(x',\,t')}{\partial x'^2} - 2c\frac{\partial^2 w(x',\,t')}{\partial x'\partial t'} - \frac{\partial^2 w(x',\,t')}{\partial t'^2} = 0\,, \tag{5}$$

i.e. the equation derived from (3) by the change of variables (4). If we normalize the coefficient of $\partial^2 w/\partial x'^2$ in (5) to 1 by another change of variables

$$x = \frac{1}{\sqrt{1-c^2}}x'\,, \quad t = t'\,, \tag{6}$$

we obtain (2), with $\nu \equiv 2c/\sqrt{1-c^2}$.

Assume that the boundary conditions (B.C.) associated with (2) are homogeneous Dirichlet:

$$w(0,\,t) = 0\,, \quad w(1,\,t) = 0\,, \quad t > 0\,. \tag{7}$$

Also, let

$$w(x,\,0) = w_0(x)\,, \quad w_t(x,\,0) = w_1(x)\,, \quad 0 < x < 1\,, \tag{8}$$

be two given initial conditions (I.C.) that are sufficiently smooth. The energy of vibration of the system at time t is defined to be

$$E(t) = \frac{1}{2}\int_0^1 [w_x^2(x,\,t) + w_t^2(x,\,t)]dx\,.$$

(This is *not* the original energy seminorm associated with (3) or (5) according to the changes of variables (4) or (6). However, it is *equivalent* to that.) Differentiating:

$$\begin{aligned}\frac{d}{dt}E(t) &= \int_0^1 [w_x w_{xt} + w_t w_{tt}]dx \\ &= \int_0^1 \frac{\partial}{\partial x}\left[w_x w_t - \frac{\nu}{2}w_t^2\right]dx \\ &= \left[w_x(x,\,t)w_t(x,\,t) - \frac{\nu}{2}w_t^2(x,\,t)\right]\Big|_{x=0}^{x=1} \\ &= 0\,,\end{aligned} \tag{9}$$

and, therefore, we see that the presence of the term $-\nu w_{xt}$ does not change the total energy of the system, i.e. energy is conserved all the time. However, there is no question that the term $-\nu w_{xt}$ is capable of *energy transport* within the system. Indeed, as we can expect from the treatment below (cf. (17)–(24)), the term $-\nu w_{xt}$ will change the speeds of wave propagation by way of which energy transport is achieved. For this reason, we give the term $-\nu w_{xt}$ a moniker *LMET*: *linear mixing energy transport*. Note that Eq. (2) is no longer invariant under the transformation (1).

Remark 1.1. There is a certain similarity between the LMET $-\nu w_{xt}$ and the *convection* term in unsteady fluid motions. Consider the 3D incompressible flow satisfying the Navier–Stokes equation without external forcing:

$$\begin{cases} \dfrac{\partial}{\partial t}\mathbf{u} + \mathbf{u}\cdot\nabla\mathbf{u} - \mu\Delta\mathbf{u} \\ \qquad + \nabla p = 0, & \text{on } \Omega, \text{ for } t > 0, \\ \nabla\cdot\mathbf{u} = 0 & \text{on } \Omega \\ \mathbf{u}|_{\partial\Omega} = \mathbf{0}, \\ \mathbf{u}(x,\,0) = \mathbf{u}_0(x), & x \in \Omega, \end{cases} \tag{10}$$

where $\mathbf{u} = \mathbf{u}(x,\,t) = (u_1(x,\,t),\, u_2(x,\,t),\, u_3(x,\,t))$ is the velocity function at point $x = (x_1,\, x_2,\, x_3) \in \Omega \subset \mathbb{R}^3$ at time t, on a bounded domain Ω with boundary $\partial\Omega$; $p = p(x,\,t)$ is the pressure function and $\mu > 0$ is a constant related to Reynold's number. The terms $\mathbf{u}\cdot\nabla\mathbf{u}$ and $-\mu\Delta\mathbf{u}$ in $(10)_1$ are called, respectively, the *convection* and *diffusion* terms. The total energy of the fluid at time t is

$$E(t) \equiv \frac{1}{2}\int_\Omega |\mathbf{u}(x,\,t)|^2 dx, \quad (dx = dx_1dx_2dx_3)\,.$$

Assume that the solution is sufficiently smooth. Then the rate of change of energy is

$$\begin{aligned}\frac{d}{dt}E(t) &= \int_\Omega \mathbf{u}\cdot\frac{\partial \mathbf{u}}{\partial t}dx\\ &= \int_\Omega \mathbf{u}\cdot[-\mathbf{u}\cdot\nabla\mathbf{u}+\mu\Delta\mathbf{u}-\nabla p]dx\\ &\quad \text{(integration by parts }\Rightarrow)\\ &= \frac{1}{2}\left\{-\int_{\partial\Omega}(\mathbf{u}\cdot\mathbf{n})|\mathbf{u}|^2 d\sigma+\int_\Omega(\nabla\cdot\mathbf{u})|\mathbf{u}|^2dx\right\}\\ &\quad -\mu\int_\Omega|\nabla\mathbf{u}|^2dx+\mu\int_{\partial\Omega}\frac{\partial\mathbf{u}}{\partial n}\cdot\mathbf{u}d\sigma\\ &\quad +\int_{\partial\Omega}(\mathbf{u}\cdot\mathbf{n})pd\sigma-\int_\Omega(\nabla\cdot\mathbf{u})pdx\,, \qquad (11)\end{aligned}$$

where $\mathbf{n}$ is the unit outward normal on $\partial\Omega$. The terms inside $\{\ldots\}$ above, contributed by the convection term $\mathbf{u}\cdot\nabla\mathbf{u}$, are equal to zero because $\mathbf{u}|_{\partial\Omega}=0$ and $\nabla\cdot\mathbf{u}=0$ on Ω. Therefore convection "transports energy around in Ω", but does not contribute to the growth or decay of the total energy. (Nevertheless, the final outcome of (11) is

$$\frac{d}{dt}E(t)=-\mu\int_\Omega|\nabla\mathbf{u}|^2dx\le 0$$

and thus, there is net energy loss due to diffusion, but not due to convection.)

The similarity between the LMET $-\nu w_{xt}$ and the convection term $\mathbf{u}\cdot\nabla\mathbf{u}$ is thence obvious as far as energy transport and conservation are concerned. This is an additional physical interpretation and motivation to our discussion in (2)–(9) above.

Remark 1.2. If the boundary condition $(10)_3$ is changed from *stationary* (i.e. $\mathbf{u}|_{\partial\Omega}=0$, the RHS of $(10)_3$) to *no-slip* (i.e. $\mathbf{u}(x,t)|_{\partial\Omega}=\mathbf{U}(x,t)$, where $\mathbf{U}(x,t)$ is the velocity of the moving boundary), then the convection term $\mathbf{u}\cdot\nabla\mathbf{u}$ in $(10)_1$ will no longer maintain a neutral role in the growth or decay of energy of fluid motion because the first term on the RHS of (11) now becomes

$$-\frac{1}{2}\int_{\partial\Omega}(\mathbf{u}\cdot\mathbf{n})|\mathbf{u}|^2d\sigma=-\frac{1}{2}\int_{\partial\Omega}(\mathbf{U}\cdot\mathbf{n})|\mathbf{u}|^2d\sigma\,,$$

which is generally indefinite in sign.

Return to the study of the wave equation. We now consider the following system of initial-boundary value problem

$$\begin{cases} w_{xx}(x,t)-\nu w_{xt}(x,t)-w_{tt}(x,t)=0, & 0<x<1, \quad t>0,\\ w_x(0,t)=0, & t>0\\ w_x(1,t)=\alpha w_t(1,t)-\beta w_t^3(1,t); & \alpha,\beta>0; \quad t>0,\\ w(x,0)=w_0(x),\ w_t(x,0)=w_1(x), & 0<x<1. \end{cases} \qquad (12)$$

In comparing the above with (2)–(8), we note that the two boundary conditions have been changed: $(12)_2$ is the homogeneous Neumann condition instead of the homogeneous Dirichlet $(7)_1$; $(12)_3$ is the self-exciting (or self-regulating) van der Pol boundary condition as we have studied in [Chen *et al.*, 1998a–1998d], which is analogous to the van der Pol ODE; see [Stoker, 1950, Chap. V.A]. Equation $(12)_3$ is the only place where nonlinearity makes its appearance. This is significant. It is also noteworthy that we need the Neumann (i.e. $(12)_2$) condition instead of the Dirichlet (i.e. $(7)_1$) in order for chaos to happen; see the explanation in Sec. 7. For now we only require α and β to be positive constants. As we make progress we will specify the range of α so that the "hysteresis" situation as in [Chen *et al.*, 1998c] can be avoided and, therefore, uniqueness of solutions of (12) is ensured.

Once again, let us examine the rate of change of energy for (12):

$$\begin{aligned}\frac{d}{dt}E(t) &= \frac{d}{dt}\left[\frac{1}{2}\int_0^1(w_x^2+w_t^2)dx\right]\\ &\quad \text{(integration by parts }\Rightarrow)\\ &= \left[w_x(x,t)w_t(x,t)-\frac{\nu}{2}w_t^2(x,t)\right]\Big|_{x=0}^{x=1}\\ &= T_1+T_2\,, \qquad (13)\end{aligned}$$

where

$$\begin{aligned}T_1 &\equiv \frac{\nu}{2}w_t^2(0,t)\,;\\ T_2 &\equiv w_t^2(1,t)\left[\left(\alpha-\frac{\nu}{2}\right)-\beta w_t^2(1,t)\right]. \qquad (14)\end{aligned}$$

Remark 1.3. The positivity or negativity of T_1 and T_2 in (14) signifies the following:

(i) $T_1 \geq 0$ if $\nu > 0$, i.e. there is *energy injection* into the system *indirectly through the LMET term* $-\nu w_{xt}$. This T_1 term would have disappeared if the homogeneous Dirichlet condition $w(0, t) = 0$ were imposed at $x = 0$; cf. Remark 1.2.

(ii) T_2 is "*regulating*" if $\alpha - (\nu/2) > 0$, i.e.

$$T_2 \geq 0 \quad \text{if} \quad |w_t(1, t)| \leq \sqrt{\frac{\alpha - \frac{\nu}{2}}{\beta}}\,;$$

$$T_2 < 0 \quad \text{if} \quad |w_t(1, t)| > \sqrt{\frac{\alpha - \frac{\nu}{2}}{\beta}}\,.$$

Thus energy is increasing if velocity is small, and decreasing if velocity is large.

(iii) T_2 is *dissipative*, i.e. $T_2 \leq 0$, if $\alpha - (\nu/2) \leq 0$.

To study (12), we now convert it into an equivalent first-order hyperbolic system: letting

$$(U, V) = (w_x, w_t)\,, \tag{15}$$

from $(12)_1$ we have

$$\frac{\partial}{\partial t}\begin{bmatrix} U \\ V \end{bmatrix} = \begin{bmatrix} 0 & 1 \\ 1 & -\nu \end{bmatrix} \frac{\partial}{\partial x}\begin{bmatrix} U \\ V \end{bmatrix} \equiv A\frac{\partial}{\partial x}\begin{bmatrix} U \\ V \end{bmatrix}. \tag{16}$$

The above hyperbolic system is not yet diagonalized. We first determine the two eigenvalues λ_1 and λ_2 and corresponding eigenvectors:

$$\lambda_1 = \rho_1(\nu) \equiv \frac{-\nu + \sqrt{4 + \nu^2}}{2} > 0\,, \quad \begin{bmatrix} 1 \\ \rho_1(\nu) \end{bmatrix};$$
$$\lambda_2 = -\rho_2(\nu) \equiv -\frac{\nu + \sqrt{4 + \nu^2}}{2} < 0\,, \quad \begin{bmatrix} 1 \\ -\rho_2(\nu) \end{bmatrix}. \tag{17}$$

Note that

$$\rho_1(\nu)\rho_2(\nu) = 1\,, \quad \rho_2(\nu) - \rho_1(\nu) = \nu > 0\,, \quad \rho_1(\nu) + \rho_2(\nu) = \sqrt{\nu^2 + 4}\,. \tag{18}$$

Let

$$P(\nu) = \begin{bmatrix} 1 & 1 \\ \rho_1(\nu) & -\rho_2(\nu) \end{bmatrix}. \tag{19}$$

Then

$$P(\nu)^{-1} = \frac{1}{\rho_1(\nu) + \rho_2(\nu)} \begin{bmatrix} \rho_2(\nu) & 1 \\ \rho_1(\nu) & -1 \end{bmatrix}. \tag{20}$$

Define

$$\begin{bmatrix} u(x, t) \\ v(x, t) \end{bmatrix} = P^{-1} \begin{bmatrix} U(x, t) \\ V(x, t) \end{bmatrix}. \tag{21}$$

Then from (16) and (19)–(21),

$$\begin{bmatrix} u \\ v \end{bmatrix}_t = P^{-1}\begin{bmatrix} U \\ V \end{bmatrix}_t = P^{-1}\left(A\begin{bmatrix} U \\ V \end{bmatrix}_x\right) = P^{-1}AP\begin{bmatrix} u \\ v \end{bmatrix}_x, \tag{22}$$

$$\begin{bmatrix} u \\ v \end{bmatrix}_t = \begin{bmatrix} \rho_1(\nu) & 0 \\ 0 & -\rho_2(\nu) \end{bmatrix}\begin{bmatrix} u \\ v \end{bmatrix}_x,$$

and thus (16) is diagonalized to (23). Note that $\rho_1(\nu)$ and $\rho_2(\nu)$ are the speeds of two families of characteristics, and they are *unequal* (if $\nu \neq 0$).

Relations (15) and (21), written in long hand, give

$$\begin{aligned} u &= \frac{1}{\rho_1(\nu) + \rho_2(\nu)}[\rho_2(\nu)w_x + w_t]\,, \\ v &= \frac{1}{\rho_1(\nu) + \rho_2(\nu)}[\rho_1(\nu)w_x - w_t]\,. \end{aligned} \tag{23}$$

The inverse relations are

$$\begin{aligned} w_x &= u + v\,, \\ w_t &= \rho_1(\nu)u - \rho_2(\nu)v\,, \end{aligned} \tag{24}$$

From (23), we can apply the method of characteristics to get

$$\begin{aligned} u(x, t) &= \phi(x + \rho_1(\nu)t)\,, \\ v(x, t) &= \psi(x - \rho_2(\nu)t)\,, \end{aligned} \tag{25}$$

for some functions ϕ and ψ (of a single variable). The above is valid for all $(x, t) \in \mathbb{R}^2$ if there were no boundary conditions imposed at $x = 0$ and $x = 1$. But we do have boundary conditions here, so (25) is not valid for all $(x, t) \in \mathbb{R}^2$ and we need to take boundary conditions into account, as given below.

The initial conditions for u and v, from $(12)_4$ and (23), are

$$u(x,\,0) = u_0(x) = \frac{1}{\rho_1(\nu)+\rho_2(\nu)}[\rho_2(\nu)w_0'(x) + w_1(x)],$$
$$v(x,\,0) = v_0(x) = \frac{1}{\rho_1(\nu)+\rho_2(\nu)}[\rho_1(\nu)w_0'(x) - w_1(x)], \qquad 0 < x < 1\,. \tag{26}$$

The boundary condition at $x = 0$, i.e. $(12)_2$, follows from $(24)_1$:

$$u(0,\,t) + v(0,\,t) = 0\,, \quad t > 0\,,$$

or

$$v(0,\,t) = -u(0,\,t) \equiv G(u(0,\,t))\,, \quad t > 0\,. \tag{27}$$

Even though $G(u) = -u$ is a simple function as defined in (27), let us stick with this seemingly more general notation G so that it may also represent other maps in Sec. 7; see (69) and (71).

The boundary condition at $x = 1$, i.e. $(12)_3$, gives

$$u + v = \alpha(\rho_1 u - \rho_2 v) - \beta(\rho_1 u - \rho_2 v)^3\,. \tag{28}$$

Denote

$$X = \rho_1 u - \rho_2 v\,. \tag{29}$$

Then (29) gives

$$u + v = \frac{1}{\rho_1}X + \frac{\rho_2}{\rho_1}v + v = \rho_2 X + (\rho_2^2+1)v\,, \tag{30}$$

and from (28) we obtain

$$\beta X^3 + (\rho_2 - \alpha)X + (\rho_2^2+1)v = 0\,. \tag{31}$$

Under the condition

$$\rho_2(\nu) - \alpha = \frac{\sqrt{4+\nu^2}+\nu}{2} - \alpha \geq 0\,, \tag{32}$$

it is known (see [Chen *et al.*, 1998a, (2.1)–(2.8)]) from Cardan's formula that for each given $v \in \mathbb{R}$, there exists a unique *real* solution $g_\nu(v)$ (a single-valued function of v) such that

$$\beta g_\nu(v)^3 + (\rho_2 - \alpha)g_\nu(v) + (\rho_2^2+1)v = 0\,; \qquad (X = g_\nu(v))\,. \tag{33}$$

On the other hand, if (32) is violated, then $g_\nu(v)$ is multivalued: for each given real v, there will exist at least one, but as many as three, real values $g_\nu(v)$ satisfying (33).

Remark 1.4. In (33), the parameter β plays the role of "scaling". This can be seen as follows. Express explicitly the dependence of $g_\nu(v)$ on β as

$$g_\nu(v) = g_\nu(v,\,\beta)\,. \tag{34}$$

We try to see if the dependence on β in (34) can somehow be "eliminated". Let us try $\beta^{\mu_1} g_\nu(\beta^{\mu_2} v,\,\beta)$ for $g_\nu(v)$ in (33):

$$\beta\cdot[\beta^{\mu_1} g_\nu(\beta^{\mu_2}v,\,\beta)]^3 + (\rho_2-\alpha)\beta^{\mu_1} g_\nu(\beta^{\mu_2}v,\,\beta) + (\rho_2^2+1)\beta^{\mu_2}v = 0\,,$$

by setting $\mu_1 = \mu_2 = -1/2$, the above becomes

$$\beta^{-1/2}[g_\nu^3 + (\rho_2-\alpha)g_\nu + (\rho_2^2+1)v] = 0\,,$$

i.e.

$$\beta^{-1/2} g_\nu(\beta^{-1/2}v,\,\beta) = g_\nu(v,\,1)\,,$$

where $g_\nu(v,\,1)$ is independent of β. The factor $\beta^{-\frac{1}{2}}$ will appear in many expressions (cf. Lemma 2.1, Lemmas 2.3–2.6, etc.) in Sec. 2. It is useful to recognize here first that $\beta^{-\frac{1}{2}}$ is just a scaling factor.

From (30), we therefore obtain an implicit representation of u in terms of v:

$$u = \rho_2[\rho_2 v + g_\nu(v)] = F_\nu(v)\,, \quad v \in \mathbb{R}\,. \tag{35}$$

From now on, without further mention, we will always assume that α, β, $\nu > 0$ also satisfy condition (32). Since $\nu > 0$, we have $\rho_2(\nu) > 1$. From (32),

$$0 < \alpha \leq \rho_2\,. \tag{36}$$

Therefore α is allowed to take values *larger than one*. (In contrast, the range of α in papers [Chen *et al.*, 1998a–1998d] was restricted to $0 < \alpha \leq 1$ in order to have the uniqueness of real solutions of cubic equations analogous to (33) therein.)

Remark 1.5. For $0 < \nu < 2$, we have

$$\rho_1(\nu) = 1 - \frac{\nu}{2} + O(\nu^2)\,, \quad \rho_2(\nu) = 1 + \frac{\nu}{2} + O(\nu^2)\,.$$

For $\nu > 2$, we have

$$\rho_1(\nu) = \frac{1}{\nu} + O(\nu^{-2})\,, \quad \rho_2(\nu) = \nu + O(1)\,.$$

Return to (23). The u-component remains constant on each characteristic $x + \rho_1(\nu)t = c =$ a positive constant, which moves leftward as t increases because $\rho_1(\nu) > 0$ by $(17)_1$. Each characteristic

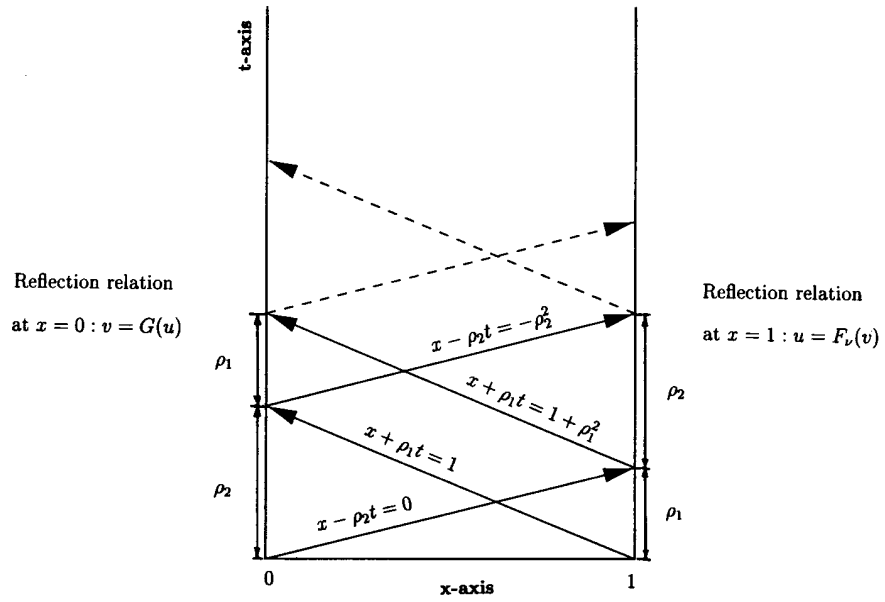

Fig. 1. Characteristics and reflection relations for the diagonalized first-order hyperbolic system (23).

as such will intersect the left boundary $x = 0$ at time $t = c/\rho_1(\nu)$, thereafter a reflection at $x = 0$ takes place. The reflection relation is precisely (27). Thus, the incoming characteristic $x+\rho_1(\nu)t = c$ and the u-component are reflected to yield an outgoing characteristic $x - \rho_2(\nu)t = -\rho_2^2(\nu)c$ moving rightward with increasing t; on this characteristic the v-component remains constant. The same can be said about reflection taking place at the right end $x = 1$, where the reflection relation is given by (35). Graphically, this is illustrated in Fig. 1.

From these reflection relations, by *ray tracing* it is straightforward to derive the following explicit representations of u and v: for $t = k(\rho_1 + \rho_2) + \tau$, $k = 0, 1, 2, \ldots$, $0 \le \tau < \rho_1 + \rho_2$ and $0 \le x \le 1$,

$$u(x, t) = \begin{cases} (F_\nu \circ G)^k(u_0(x + \rho_1\tau)), & \tau \le \rho_2(1 - x)\,, \\ F_\nu \circ (G \circ F_\nu)^k(v_0(1 + \rho_2^2 - \rho_2^2(x + \rho_1\tau))), & \rho_2(1 - x) < \tau \le \rho_2(1 + \rho_1^2 - x)\,, \\ (F_\nu \circ G)^{k+1}(u_0(x + \rho_1\tau - 1 - \rho_1^2)), & \rho_2(1 + \rho_1^2 - x) < \tau < \rho_1 + \rho_2\,, \end{cases} \tag{37}$$

$$v(x, t) = \begin{cases} (G \circ F_\nu)^k(v_0(x - \rho_2\tau)), & \tau \le \rho_1 x \\ G \circ (F_\nu \circ G)^k(u_0(-\rho_1^2(x - \rho_2\tau)))\,, & \rho_1 x < \tau \le \rho_1(x + \rho_2^2)\,, \\ (F_\nu \circ G)^{k+1}(v_0(x - \rho_2\tau + 1 + \rho_2^2))\,, & \rho_1(x + \rho_2^2) < \tau < \rho_1 + \rho_2\,. \end{cases} \tag{38}$$

Note that in the above, for example, $(G \circ F_\nu)^k$ denotes the k-times iterative composition of $G \circ F_\nu$ with itself (rather than the kth power of the function $G \circ F_\nu$). From these explicit representations, we see that the u-component and/or the v-component show(s) chaotic behavior if and only if the map(s) $G \circ F_\nu$ and/or $F_\nu \circ G$ is/are chaotic. We will make more precise what we mean by being chaotic or nonchaotic *of the system* (*12*) from that of u and v based upon certain *topological conjugacy*; see Sec. 5.

The organization of the paper is given as follows. In Sec. 2, we list various basic properties of the map $G \circ F_\nu$. In Sec. 3, we establish the route to chaos: period-doubling, homoclinic orbits and bifurcations, and invariant Cantor sets. In Sec. 4, we prove the topological conjugacy between (u, v) and (w_x, w_t). In Sec. 5, we examine the differentiability of the solution, from which chaotic behavior of w itself may also be deduced. Numerical simulations of chaotic vibration are given in Sec. 6. Additional discussions are made in the final Sec. 7.

2. Basic Properties of the Map $G \circ F_\nu$

It is easy to check that F_ν is odd: $F_\nu(-v) = -F_\nu(v)$.

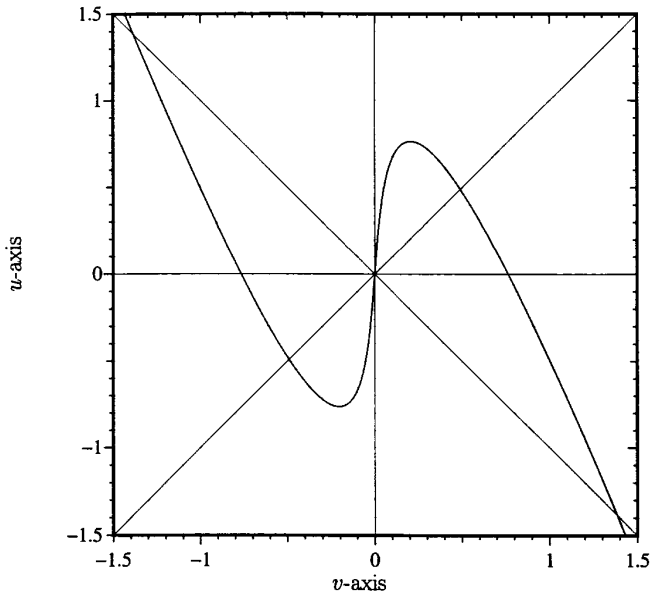

Fig. 2. The graph of $u = GF_\nu(v)$, with $\alpha = 4/3$, $\beta = 1$, $\nu = 1.24$.

Also, because $G(v) = -v$, we see that $G \circ F_\nu(v) = F_\nu \circ G(v) = -F_\nu(v)$. Therefore, in (37) and (38) investigation of the periodic and chaotic behavior of $G \circ F_\nu$ alone suffices here because $F_\nu \circ G$ is the same function. Throughout most of the discussion in this section, we will regard α, β as given fixed constants, and ν as a varying parameter.

As a visual aid, we first plot a graph of $G \circ F_\nu$ in Fig. 2, for $\alpha = 4/3$, $\beta = 1$ and $\nu = 1.24$. Let us begin to analyze the properties of $G \circ F_\nu$, below.

Lemma 2.1 (Fixed Points). *Let $\nu > 0$, $0 < \alpha \leq \rho_2(\nu)$ and $\beta > 0$. Then $G \circ F_\nu$ has exactly three fixed points 0, v_0 and $-v_0$, where $v_0 = v_0(\nu) = [1/(\rho_1 + \rho_2)]\sqrt{\alpha/\beta}$.*

Proof. If

$$\begin{aligned} v_0 &= G \circ F_\nu(v_0) = -F_\nu(v_0) \\ &= -\rho_2^2 v_0 - \rho_2 g_\nu(v_0)\,, \end{aligned}$$

then

$$g_\nu(v_0) = -\frac{1}{\rho_2}(1+\rho_2^2)v_0 = -(\rho_1+\rho_2)v_0\,, \quad (39)$$

and by (33),

$$-\beta(\rho_1+\rho_2)^3 v_0^3 - (\rho_1+\rho_2)(\rho_2-\alpha)v_0 + (\rho_2^2+1)v_0 = 0\,,$$

$$\begin{aligned} \beta(\rho_1+\rho_2)^3 v_0^2 &= \rho_2^2 + 1 - (\rho_1+\rho_2)(\rho_2-\alpha) \\ &= \alpha(\rho_1+\rho_2) > 0\,. \end{aligned}$$

Hence

$$v_0 = \pm\frac{1}{\rho_1+\rho_2}\sqrt{\frac{\alpha}{\beta}}\,. \quad (40)$$

■

Note that the graph of $u = G \circ F_\nu(v)$ intersects the diagonal $u - v = 0$ at exactly the three points $(-v_0, -v_0)$, $(0, 0)$ and (v_0, v_0).

Lemma 2.2 (Derivative Formulas). *Let $\nu > 0$, $0 < \alpha \leq \rho_2(\nu)$, $\beta > 0$, where ν is a varying parameter but α and β are given and fixed (as long as $\alpha \in (0, \rho_2(\nu)]$). Define $f(v, \nu) = G \circ F_\nu(v) = -\rho_2(\nu)[\rho_2(\nu)v + g_\nu(v)]$, where g_ν is defined through (33). Then*

$$\frac{\partial}{\partial v} f(v,\nu) = -\rho_2^2 + \rho_2 \cdot \frac{\rho_1^2+1}{D}\,, \quad (41)$$

$$\begin{aligned} \frac{\partial}{\partial \nu} f(v,\nu) &= -\rho_2'[2\rho_2 v + g_\nu(v)] \\ &\quad + \rho_2\rho_2' \cdot \frac{2\rho_2 v + g_\nu(v)}{D}\,, \end{aligned} \quad (42)$$

$$\begin{aligned} \frac{\partial^2}{\partial\nu\partial v} f(v,\nu) &= -\rho_2'\left(2\rho_2 - \frac{\rho_2^2+1}{D}\right) \\ &\quad + \rho_2\rho_2'\Bigg[\frac{2\rho_2 D - (\rho_2^2+1)}{D^2} \\ &\quad + \frac{6\beta(\rho_2^2+1)(2\rho_2 v + g_\nu(v))g_\nu(v)}{D^3}\Bigg]\,, \end{aligned} \quad (43)$$

$$\frac{\partial^2}{\partial v^2} f(v,\nu) = \frac{6\beta\rho_2(\rho_2^2+1)^2 g_\nu(v)}{D^3}\,, \quad (44)$$

$$\frac{\partial^3}{\partial v^3} f(v,\nu) = \frac{24\beta\rho_2(\rho_2^2+1)^4}{D^4}\,, \quad (45)$$

where

$$D = D(v,\nu,\alpha,\beta) = 3\beta g_\nu^2(v) + \rho_2 - \alpha\,,$$

$$\rho_2' = \rho_2'(\nu) = \frac{\nu + \sqrt{4+\nu^2}}{2\sqrt{4+\nu^2}}\,.$$

Proof. We will only verify (41); the rest can be done in a similar way. By the definition of $f(v, \nu)$, we have

$$\frac{\partial}{\partial v} f(v,\nu) = -\rho_2^2 - \rho_2 g_\nu'(v)\,. \quad (46)$$

By differentiating (33) with respect to v, we get

$$3\beta g_\nu^2(v)g_\nu'(v) + (\rho_2 - \alpha)g_\nu'(v) + (\rho_2^2 + 1) = 0\,,$$

$$g_\nu'(v) = -\frac{\rho_2^2 + 1}{3\beta g_\nu^2(v) + \rho_2 - \alpha}\,. \tag{47}$$

Substitution of (47) into (46) gives us (41). ■

Corollary 2.1. *The origin is a repelling fixed point of the map $G \circ F_\nu$.*

Proof. At $v = 0$, we have $g_\nu(0) = 0$ and $g_\nu'(0) = -(\rho_2^2 + 1)/(\rho_2 - \alpha) < 0$. By (46) and (47),

$$[G \circ F_\nu]'(0) = -\rho_2^2 + \frac{\rho_2^3 + \rho_2}{\rho_2 - \alpha} = \frac{\rho_2(\alpha\rho_2 + 1)}{\rho_2 - \alpha}$$

$$= 1 + \frac{\alpha(1 + \rho_2^2)}{\rho_2 - \alpha} > 1\,. \quad ■$$

Lemma 2.3 (Local Maximum, Minimum and Piecewise Monotonicity). *Let $\nu > 0$, $0 < \alpha \le \rho_2(\nu)$, and $\beta > 0$ be given. Then $G \circ F_\nu$ has local extremal values*

$$m = G \circ F_\nu(-v_c) = -\frac{2}{3}\frac{1 + \alpha\rho_2}{\rho_1 + \rho_2}\sqrt{\frac{1 + \alpha\rho_2}{3\beta\rho_2}}\,,$$

$$M = G \circ F_\nu(v_c) = \frac{2}{3}\frac{1 + \alpha\rho_2}{\rho_1 + \rho_2}\sqrt{\frac{1 + \alpha\rho_2}{3\beta\rho_2}} = -m\,, \tag{48}$$

where

$$v_c = \frac{3\rho_2^2 - 2\alpha\rho_2 + 1}{3\rho_2(\rho_2^2 + 1)}\sqrt{\frac{1 + \alpha\rho_2}{3\beta\rho_2}} \quad \textit{and} \quad -v_c$$

are critical points of $G \circ F_\nu$, and m, M are, respectively, the local minimum and maximum of $G \circ F_\nu$. The function $G \circ F_\nu$ is strictly decreasing on $(-\infty, -v_c)$ and (v_c, ∞), but strictly increasing on $(-v_c, v_c)$.

Proof. Use (41), (35), etc., and carry out the computations. ■

Lemma 2.4 (v-Axis Intercepts). *Let $\nu > 0$, $0 < \alpha \le \rho_2(\nu)$, and $\beta > 0$ be given. Then $u = G \circ F_\nu(v)$ intersects the v-axis at abscissas $\pm v_I$, where $v_I = (1/\rho_2)\sqrt{(1 + \alpha\rho_2)/\beta\rho_2}$.*

Proof. Set $G \circ F_\nu(v_I) = 0$ and solve for v_I. ■

Lemma 2.5 (Intersections with the Diagonal Line $u + v = 0$). *Let $\nu > 0$, $0 < \alpha \le \rho_2(\nu)$ and $\beta > 0$ be given. Then the graph of $u = G \circ F_\nu(v)$ intersects the line $u + v = 0$ at exactly the following three points*:

$$(-\tilde{v},\, \tilde{v}), \quad (0,\, 0), \quad (\tilde{v},\, -\tilde{v})\,,$$

where

$$\tilde{v} = \tilde{v}(\nu) = \frac{1}{\rho_2 - \rho_1}\sqrt{\frac{1 + \alpha(\rho_2 - \rho_1)}{\beta(\rho_2 - \rho_1)}}\,.$$

Proof. Set $G \circ F_\nu(\tilde{v}) = -\tilde{v}$ and solve for $\tilde{v}$. ■

Lemma 2.6 (Bounded Invariant Interval $\mathcal{I}$). *Let $\nu > 0$, $0 < \alpha \le \rho_2(\nu)$ and $\beta > 0$ be given, such that*

$$M = \frac{2}{3}\frac{1 + \alpha\rho_2}{\rho_1 + \rho_2}\sqrt{\frac{1 + \alpha\rho_2}{3\beta\rho_2}} \le \tilde{v}$$

$$= \frac{1}{\rho_2 - \rho_1}\sqrt{\frac{1 + \alpha(\rho_2 - \rho_1)}{\beta(\rho_2 - \rho_1)}}\,. \tag{49}$$

Then the iterates of every point in the set $U \equiv (-\infty, \tilde{v}) \cup (\tilde{v}, \infty)$ by $G \circ F_\nu$ escape to $\pm\infty$, while $\mathcal{I} \equiv \mathbb{R}\backslash\overline{U} = [-\tilde{v}, \tilde{v}]$ is an invariant interval of $G \circ F_\nu$.

Proof. Obvious; see Fig. 2, for example. ■

The set U in Lemma 2.6 is the unstable set, and the set $\mathcal{I}$ is the bounded invariant set. When the condition (49) is violated, bounded invariant interval $\mathcal{I}$ no longer exists. Instead, we have a bounded Cantor-like invariant set; see Sec. 3.

3. Routes to Chaos

First, we show that there is a period-doubling cascade.

Theorem 3.1 (Period-Doubling Bifurcation Theorem for the Map $G \circ F_\nu$). *Let $\alpha, \beta > 0$ be given such that $0 < \alpha \le \sqrt{2}$. Define $\overline{\nu}_{1,\alpha}$ by*

$$\overline{\nu}_{1,\alpha} = \begin{cases} \varepsilon, & \text{if } 0 < \alpha < 1, \text{ where } \varepsilon \text{ is any small positive number,} \\ r, & \text{if } \alpha \ge 1, \text{ where } r \text{ is the unique positive solution of } \rho_2(r) = \alpha\,. \end{cases} \tag{50}$$

Let $\nu \in [\overline{\nu}_{1,\alpha}, \infty)$ be a varying parameter. Define $f(v, \nu) = GF_\nu(v)$. Then

(i) α *satisfies* $0 < \alpha \le \rho_2(\nu)$ *for all* $\nu \in [\overline{\nu}_{1,\alpha}, \infty)$.

(ii) $v_0(\nu) = [1/(\rho_1(\nu) + \rho_2(\nu)]\sqrt{\alpha/\beta}$ *is a curve of fixed points of* $f : f(v_0(\nu), \nu) = v_0(\nu)$.

(iii) *For* $\nu_0 = 1/\alpha$, *we have* $\nu_0 > \overline{\nu}_{1,\alpha}$, $\rho_2(\nu_0) \ge \alpha$, *and*

$$\frac{\partial}{\partial v} f(v, \nu)|_{\substack{v=v_0(\nu)\\ \nu=\nu_0}} = -1\,. \tag{51}$$

(iv) *For* $\nu = \nu_0 = 1/\alpha$ *and* $v = v_0(\nu)$, *we have*

$$A \equiv \left[\frac{\partial^2 f}{\partial \nu \partial v} + \frac{1}{2}\left(\frac{\partial f}{\partial \nu}\right)\frac{\partial^2 f}{\partial v^2}\right]\Bigg|_{\substack{v=v_0(\nu)\\ \nu=\nu_0}} \neq 0\,. \tag{52}$$

(v) *For* $\nu = \nu_0 = 1/\alpha$ *and* $v = v_0(\nu)$, *we have*

$$B = \left[\frac{1}{6}\frac{\partial^3 f}{\partial v^3} + \frac{1}{4}\left(\frac{\partial^2 f}{\partial v^2}\right)^2\right]\Bigg|_{\substack{v=v_0(\nu)\\ \nu=\nu_0}} > 0\,.$$

Consequently, there is period-doubling bifurcation at $(v, \nu) = (v_0(\nu), 1/\alpha)$. *The stability type of the bifurcated period-2 orbit is attracting.*

Proof

(i) Since $\rho_2(\nu) = [\sqrt{\nu^2 + 4} + \nu]/2$ is an increasing function of ν with range $[1, \infty)$, we see that if $\alpha \ge 1$, $\rho_2(\nu) = \alpha$ has a unique positive solution $\overline{\nu}_{1,\alpha}$ such that $\rho_2(\nu) \ge \alpha$ if $\nu \ge \overline{\nu}_{1,\alpha}$.

(ii) See Lemma 2.1.

(iii) Let us find ν_0 satisfying (51):

$$\begin{aligned}\frac{\partial}{\partial v} f(v, \nu)|_{\substack{v=v_0(\nu)\\ \nu=\nu_0}} &= -\rho_2^2 - \rho_2 g'_{\nu_0}(v_0(\nu_0))\\ &= -1\,,\end{aligned}$$

or

$$\begin{aligned} g'_{\nu_0}(v_0(\nu_0)) &= \frac{1}{\rho_2}(1 - \rho_2^2) = \rho_1 - \rho_2\\ &= -\frac{\rho_2^2 + 1}{3\beta g_{\nu_0}^2(v_0(\nu_0)) + \rho_2 - \alpha} \qquad \text{(by (47))}\\ &= -\frac{\rho_2^2 + 1}{3\beta\left[-(\rho_1 + \rho_2)\cdot\dfrac{1}{\rho_1 + \rho_2}\sqrt{\dfrac{\alpha}{\beta}}\right]^2 + \rho_2 - \alpha} \qquad \text{(by (39), (40))}\\ &= -\frac{\rho_2^2 + 1}{\rho_2 + 2\alpha}\,, \end{aligned} \tag{53}$$

$$\begin{aligned} \rho_1 - \rho_2 &= -\frac{\rho_2^2 + 1}{\rho_2 + 2\alpha} = -\frac{\rho_1 + \rho_2}{1 + 2\alpha\rho_1}\,,\\ \nu_0 &= \frac{\sqrt{4 + \nu_0^2}}{1 + \alpha(\sqrt{4 + \nu_0^2} - \nu_0)}\,, \quad \nu_0 = \frac{1}{\alpha}\,. \end{aligned} \tag{54}$$

(iv) We substitute (42)–(44) into the defining equation (52) for A. Note from (iii) above that we have

$$\nu_0 = \frac{1}{\alpha}\,, \quad g_{\nu_0}(v_0(\nu_0)) = -\sqrt{\frac{\alpha}{\beta}}\,,$$

$$v_0(\nu_0) = \frac{\sqrt{\dfrac{\alpha}{\beta}}}{\rho_1(\nu_0) + \rho_2(\nu_0)}\,, \quad \text{(by (40))}$$

$$D = 2\alpha + \frac{\sqrt{\nu_0^2 + 4} + \nu_0}{2} = \rho_2(\nu_0) + 2\alpha\,,$$

$$\rho'_2(\nu_0) = \frac{\rho_2(\nu_0)}{\rho_1(\nu_0) + \rho_2(\nu_0)}\,,$$

$$2\rho_2(\nu_0)v_0(\nu_0) + g_{\nu_0}(v_0(\nu_0)) = \nu_0 v_0(\nu_0)\,.$$

We can substitute all of the above into (42)–(44), obtaining $A = A(\alpha)$, i.e. A is *independent of* β. We plot the graph of $A(\alpha)$ against $\alpha : 0 < \alpha \le \sqrt{2}$ in Fig. 3 and found that $A(\alpha) < 0$ for any given $\alpha > 0$. (This part of the proof is computer-assisted.)

(v) This is obvious because $\partial^3 f/\partial v^3 > 0$ from (45). ■

The graph of $G \circ F_\nu$ is *unimodal* for $v \geq 0$. Through the *renormalization* argument of [Feigenbaum, 1978] and [Collet & Tresser, 1962], we see that once period-doubling occurs, it will repeat as a cascade, leading to chaos.

The period-doubling cascade of $G \circ F_\nu$ can be seen in Fig. 4 for $\alpha = 1/2$ and $\beta = 1$.

If the condition $0 < \alpha \leq \sqrt{2}$ in Theorem 3.1 is violated, then there is still period doubling, except that the first period doubling occurs on period-2 orbits, making them into period-4 orbits, such as shown in Fig. 5. If α keeps increasing, then the first period doubling occurs on period-2^n orbits for some larger n.

Next, we show the existence of homoclinic orbits.

Theorem 3.2 (Homoclinic Orbits). *Define*

$$h(\rho_2(\nu)) = \frac{1}{1+\alpha\rho_2}\left(1+\frac{1}{\rho_2^2}\right) = \frac{1}{1+\alpha\rho_2(\nu)}\left(1+\frac{1}{\rho_2^2(\nu)}\right) \quad (55)$$

and let $\overline{\nu}_{2,\alpha}$ be the unique positive solution of $h(\rho_2(\nu)) = 2/3\sqrt{3}$. Assume that either

(i) $\alpha > 3\sqrt{3} - 1$ *and* $\nu \geq \overline{\nu}_{1,\alpha}$, *or*

(ii) $0 < \alpha \leq 3\sqrt{3}-1$ *and* $\nu > \min(\overline{\nu}_{1,\alpha}, \overline{\nu}_{2,\alpha})$, *where* $\overline{\nu}_{1,\alpha}$ *is defined as in* (*50*).

Then the repelling fixed point 0 of the map $G \circ F_\nu$ has nondegenerate homoclinic orbits. Furthermore, if $\nu = \overline{\nu}_{2,\alpha} \geq \overline{\nu}_{1,\alpha}$ then the fixed point 0 has degenerate homoclinic orbits.

Proof. Homoclinic orbits exist near the origin if $M > v_I$; cf. Lemmas 2.3 and 2.4 for notation. (The concept of a homoclinic orbit is very much *geometric* in nature. This enables an easy visual confirmation from a graph such as Fig. 2.) Thus

$$M > v_I \quad \text{if and only if} \quad \frac{2}{3}\frac{1+\alpha\rho_2}{\rho_1+\rho_2}\sqrt{\frac{1+\alpha\rho_2}{3\beta\rho_2}} > \frac{1}{\rho_2}\sqrt{\frac{1+\alpha\rho_2}{\beta\rho_2}},$$

or, after simplifying,

$$\frac{2}{3\sqrt{3}} > \frac{1}{1+\alpha\rho_2}\left(1+\frac{1}{\rho_2^2}\right). \quad (56)$$

The RHS of (56) is the function h in (55) which is a decreasing function of ρ_2 and, hence, is also a

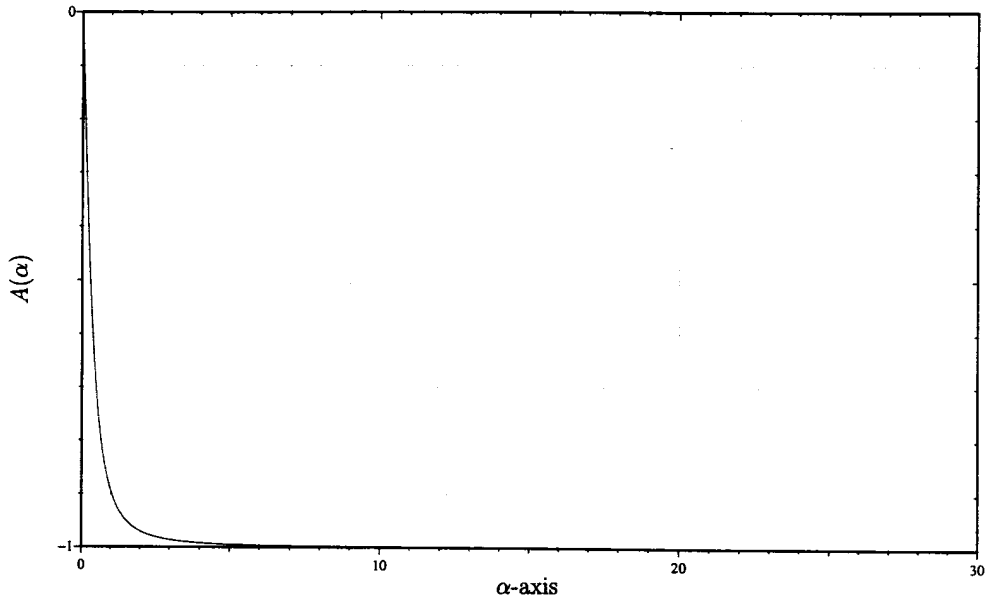

Fig. 3. The graph of $A = A(\alpha)$, cf. (52), as a function of α. Note that $A(\alpha)$ is negative for any $\alpha \geq 0$.

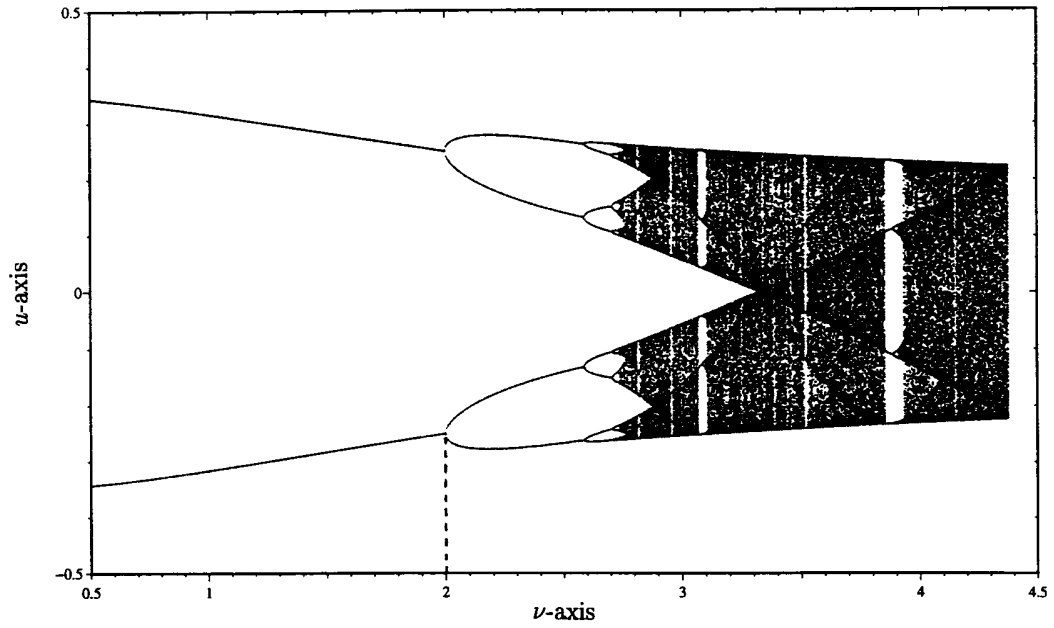

Fig. 4. The orbit diagram of GF_ν for $\alpha = 1/2$, $\beta = 1$. Note that the first period doubling occurs at $\nu = 2$, agreeing with (54) of Theorem 3.1.

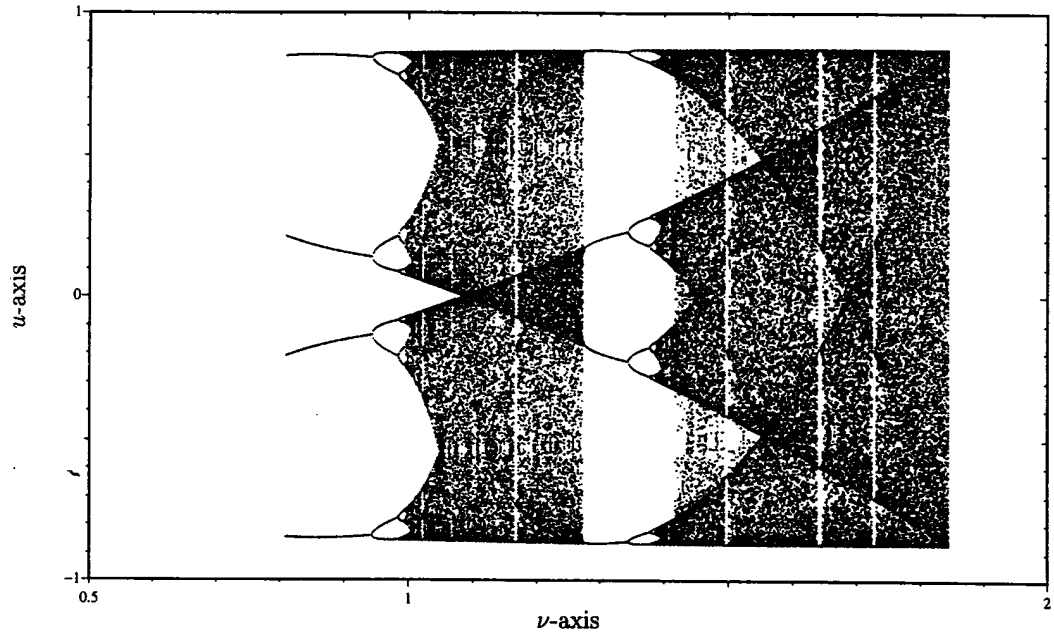

Fig. 5. The orbit diagram of $G \circ F_\nu$ for $\alpha = 1.5$, $\beta = 1$. Note that $\alpha > \sqrt{2}$ here, and the first period doubling occurs on a period-4 orbit.

decreasing function of the variable ν. On $[0, \infty)$, $h \circ \rho_2$ takes its minimum at $\nu = 0$:

$$h(\rho_2(0)) = \frac{1}{1+\alpha\rho_2(0)}\left(1+\frac{1}{\rho_2^2(0)}\right) = \frac{2}{1+\alpha}\,.$$

If α satisfies

$$\frac{2}{3\sqrt{3}} > \frac{2}{1+\alpha}\,, \quad \text{i.e.} \quad \alpha > 3\sqrt{3}-1\,,$$

then (56) is satisfied for all $\nu \geq \overline{\nu}_{1,\alpha}$. There then exist nondegenerate homoclinic orbits.

On the other hand, if α satisfies

$$\frac{2}{3\sqrt{3}} < \frac{2}{1+\alpha},$$

then there exists a unique $\overline{\nu}_{2,\alpha} > 0$ such that $h(\rho_2(\nu)) = 2/3\sqrt{3}$. Therefore, if $\nu > \min(\overline{\nu}_{1,\alpha}, \overline{\nu}_{2,\alpha})$, then nondegenerate homoclinic orbits also exist.

Degenerate homoclinic orbits (and, consequently, *homoclinic bifurcations*) arise when $M = v_I$. This happens if and only if $\nu = \overline{\nu}_{2,\alpha} \geq \overline{\nu}_{1,\alpha}$. ■

Proposition 3.1. *For α, β, $\nu > 0$, let*

$$M_\nu \equiv \frac{2}{3}\frac{1+\alpha\rho_2(\nu)}{\rho_1(\nu)+\rho_2(\nu)}\sqrt{\frac{1+\alpha\rho_2(\nu)}{3\beta\rho_2(\nu)}}$$

be the local maximum of $G \circ F_\nu$ as given in (48), and let

$$\tilde{v}(\nu) \equiv \frac{1}{\rho_2(\nu)\rho_1(\nu)}\sqrt{\frac{1+\alpha[\rho_2(\nu)-\rho_1(\nu)]}{\beta[\rho_2(\nu)-\rho_1(\nu)]}}$$

be the value of intersection of $G \circ F_\nu$ with $u+v=0$ as given in Lemma 2.5. Then for each given α, $\beta > 0$, there exists a unique $\tilde{\nu}(\alpha)$, dependent on α but independent of β, such that $\rho_2(\tilde{\nu}(\alpha)) > \alpha$, $\tilde{\nu}(\alpha)$ is strictly decreasing with respect to α, and

$$M_\nu = \tilde{v}(\nu)|_{\nu=\tilde{\nu}(\alpha)}.$$

Also,

$$M_\nu > \tilde{v}(\nu) \quad \text{for } \nu > \tilde{\nu}(\alpha).$$

Proof. It is easy to verify that as a function of ν, $\tilde{v}(\nu)$ is strictly decreasing, for fixed α and β. However, as a function of ν, M_ν is not monotonic with respect to ν in general. This makes the mathematical analysis more involved. Here, we simply provide a computer-assisted proof by numerically solving $M_\nu = \tilde{v}(\nu)$ to determine the dependence of ν on α. The graph of $\nu = \tilde{\nu}(\alpha)$ is plotted in Fig. 6. The conclusion follows. ■

Corollary 3.1 (Homoclinic Orbits and Ensuing Chaos on the Bounded Invariant Interval $\mathcal{I}$). *Given α, $\beta > 0$, let $\nu > 0$ satisfy*

(i) *$\alpha > 3\sqrt{3}-1$ and $\nu \geq \overline{\nu}_{1,\alpha}$ or $0 < \alpha \leq 3\sqrt{3}-1$ and $\nu > \min(\overline{\nu}_{1,\alpha}, \overline{\nu}_{2,\alpha})$, where $\overline{\nu}_{1,\alpha}$ and $\overline{\nu}_{2,\alpha}$ are given in Theorems 3.1 and 3.2;*

(ii) *$\nu \leq \tilde{\nu}(\alpha)$, where $\tilde{\nu}(\alpha)$ is given in Proposition 3.1.*

Let $\mathcal{I} = [-\tilde{v}, \tilde{v}]$ be the bounded invariant interval corresponding to ν as given in Lemma 2.6. Then $G \circ F_\nu : \mathcal{I} \to \mathcal{I}$ is chaotic.

When $\nu > \tilde{\nu}(\alpha)$, $G \circ F_\nu$ no longer has a bounded invariant interval. An exemplar graph of

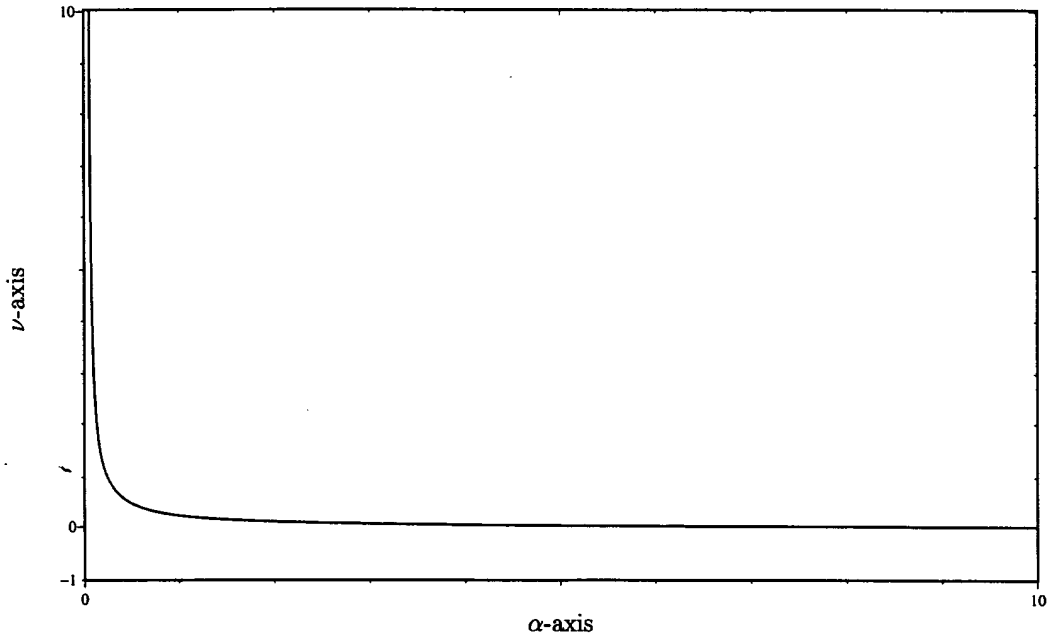

Fig. 6. The graph of $\nu = \tilde{\nu}(\alpha)$ in Proposition 3.1.

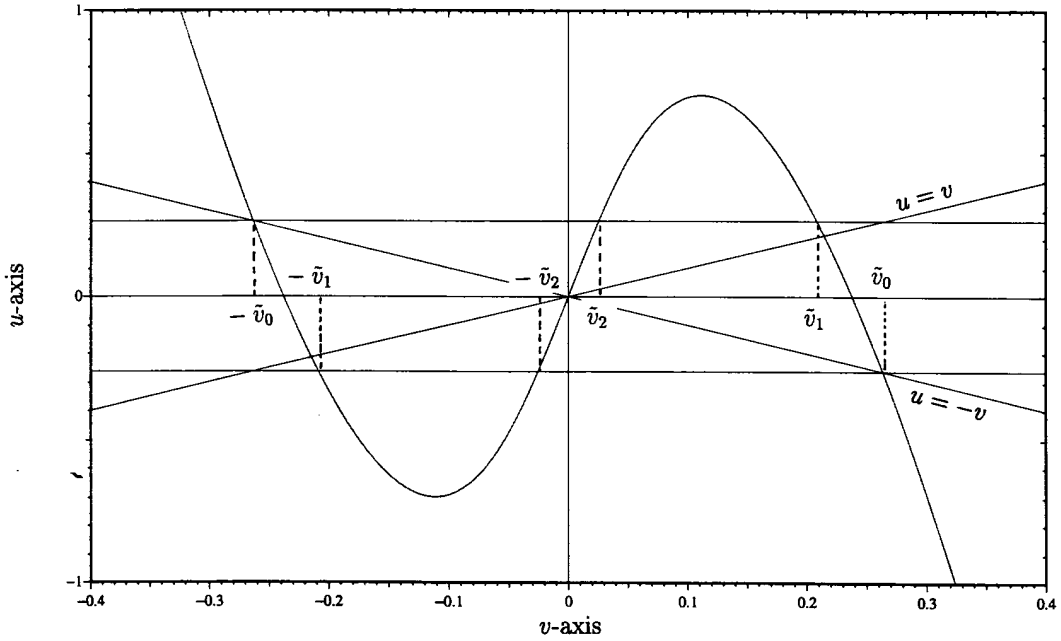

Fig. 7. The graph of $G \circ F_\nu$ for $\alpha = 4/3$, $\beta = 1$, $\nu = 5$.

the map $G \circ F_\nu$ is illustrated in Fig. 7. The two horizontal lines $u = \pm\tilde{v}(\nu)$ intersect the graph of $u = G \circ F_\nu(v)$ at a total of six points, as can be seen from Fig. 7. We denote the ordered abscissas of these six points by

$$-\tilde{v}_0 \equiv -\tilde{v}(\nu),\ -\tilde{v}_1,\ -\tilde{v}_2,\ \tilde{v}_2,\ \tilde{v}_1,\ \tilde{v}_0\,,$$

where $\tilde{v}_1$ and $\tilde{v}_2$ are defined uniquely through

$$0 < \tilde{v}_2 < \tilde{v}_1 < \tilde{v}_0$$

$$= \tilde{v}(\nu) = \frac{1}{\rho_2(\nu) - \rho_1(\nu)} \sqrt{\frac{1 + \alpha \cdot (\rho_2(\nu) - \rho_1(\nu))}{\beta \cdot (\rho_2(\nu) - \rho_1(\nu))}}\,,$$

$$G \circ F_\nu(\tilde{v}_1)$$

$$= G \circ F_\nu(\tilde{v}_2)$$

$$= \frac{1}{\rho_2(\nu) - \rho_1(\nu)} \sqrt{\frac{1 + \alpha \cdot (\rho_2(\nu) - \rho_1(\nu))}{\beta \cdot (\rho_2(\nu) - \rho_1(\nu))}}\,.$$

We then define five intervals

$$I_0 = [-\tilde{v}_0,\ -\tilde{v}_1]\,, \quad I_1 = [-\tilde{v}_2,\ \tilde{v}_2]\,, \quad I_2 = -I_0\,,$$
$$A_0 = (-\tilde{v}_1,\ -\tilde{v}_2)\,, \quad A_1 = -A_0\,.$$

It is easy to see that

$$v \in \mathcal{I} = [-\tilde{v}_0,\ \tilde{v}_0], \quad (G \circ F_\nu)^n(v) \in A_0 \cup A_1 \text{ for some } n \in \{0,\ 1,\ 2, \ldots\}$$
$$\Rightarrow \lim_{k \to \infty} |(G \circ F_\nu)^n(v)| = \infty\,.$$

The set

$$\Lambda = \bigcap_{n=0}^{\infty} (G \circ F_\nu)^{-n} \mathcal{I} \tag{57}$$

is a closed bounded invariant subset of the map $G \circ F_\nu$. For every $v \in \Lambda$, we can assign an itinerary $s(v)$ of v by

$$s(v) = (s_0\ s_1 s_2 \cdots s_n \cdots)$$

$$s_n = \left\{ \begin{matrix} 0 \\ 1 \\ 2 \end{matrix} \right\} \text{ if } (G \circ F_\nu)^n v \in \left\{ \begin{matrix} I_0 \\ I_1\,, \\ I_2 \end{matrix} \right. \quad n = 0,\ 1,\ 2, \ldots.$$

Then $s(v)$ is a ternary number. We have $s(v) \in \sum_3$, where

$$\sum_3 = \{s = (s_0\ s_1 s_2 \cdots s_n \cdots) | s_j = 0,\ 1 \text{ or } 2, \text{ for } j = 0,\ 1,\ 2, \ldots\}\,.$$

$\sum_3$ is endowed with a natural metric for ternary numbers. Then standard techniques in symbolic dynamics (see [Devaney, 1989; Robinson, 1995, pp. 33–37], e.g.) give us the following.

Theorem 3.3 (Chaos on Cantor-Like Invariant Set Λ). *For given α, $\beta > 0$, let $\nu > \tilde{\nu}(\alpha)$. Then Λ defined in (57) is a Cantor set with measure zero, and the map $G \circ F_\nu$ on Λ is topologically conjugate*

to the shift map on $\sum_3$. Consequently, $G \circ F_\nu$ is chaotic on Λ.

4. Topological Conjugacy Between (u, v) and (w_x, w_t)

In Sec. 3, we have determined the parameter ranges in which u and v components display several types of chaotic behavior. In this section, we show that the gradient (w_x, w_t) is topologically conjugate to (u, v) and, therefore, is chaotic if and only if (u, v) is. The proof given below is a generalization of the one in [Chen *et al.*, 1998a, Sec. 5].

From the reflection of characteristics as shown in Fig. 2 and from (24), for any $t \geq 0$, we have

$$\begin{aligned} w_x(1, t + (\rho_1 + \rho_2)) &= u(1, t + (\rho_1 + \rho_2)) + v(1, t + (\rho_1 + \rho_2)) \\ &= F_\nu(v(1, t + (\rho_1 + \rho_2)) - u(0, t + \rho_2) \\ &= F_\nu(-u(0, t + \rho_2)) - u(0, t + \rho_2) \\ &= F_\nu(-u(1, t)) - u(1, t) \\ &= \left[-\frac{\rho_2}{\rho_1 + \rho_2} w_x(1, t) - \frac{1}{\rho_1 + \rho_2} w_t(1, t)\right] \\ &\quad + F_\nu\left(-\frac{\rho_2}{\rho_1 + \rho_2} w_x(1, t) - \frac{1}{\rho_1 + \rho_2} w_t(1, t)\right). \end{aligned}$$

Similarly,

$$\begin{aligned} w_t(1, t + (\rho_1 + \rho_2)) &= \rho_1 u(1, t + (\rho_1 + \rho_2)) - \rho_2 v(1, t + (\rho_1 + \rho_2)) \\ &= \rho_2 \left[\frac{\rho_2}{\rho_1 + \rho_2} w_x(1, t) + \frac{1}{\rho_1 + \rho_2} w_t(1, t)\right] \\ &\quad + \rho_1 F_\nu\left(-\frac{\rho_2}{\rho_1 + \rho_2} w_x(1, t) - \frac{1}{\rho_1 + \rho_2} w_t(1, t)\right). \end{aligned}$$

Write the above as a 2×2 iterative system

$$\begin{bmatrix} \xi_{n+1} \\ \eta_{n+1} \end{bmatrix} = \begin{bmatrix} -\left(\frac{\rho_2}{\rho_1 + \rho_2}\xi_n + \frac{1}{\rho_1 + \rho_2}\eta_n\right) + GF_\nu\left(\frac{\rho_2}{\rho_1 + \rho_2}\xi_n + \frac{1}{\rho_1 + \rho_2}\eta_n\right) \\ \rho_2\left(\frac{\rho_2}{\rho_1 + \rho_2}\xi_n + \frac{1}{\rho_1 + \rho_2}\eta_n\right) + \rho_1 GF_\nu\left(\frac{\rho_2}{\rho_1 + \rho_2}\xi_n + \frac{1}{\rho_1 + \rho_2}\eta_n\right) \end{bmatrix}, \tag{58}$$

where

$$\begin{aligned} \xi_n &= w_x(1, t_0 + n(\rho_1 + \rho_2)), \\ \eta_n &= w_t(1, t_0 + n(\rho_1 + \rho_2)), \\ n &\geq 0, \quad t_0 \in [0, \rho_1 + \rho_2). \end{aligned}$$

We now show that (58) is topologically conjugate to the one-dimensional iterative map $v_{n+1} = GF_\nu(v_n)$.

Define a set

$$\begin{aligned} \mathcal{C} = \{(\xi, \eta) \in \mathbb{R}^2 | &\xi = -c + GF_\nu(c), \\ &\eta = \rho_2 c + \rho_1 GF_\nu(c), \forall\, c \in \mathbb{R}\}. \end{aligned}$$

Then $\mathcal{C}$ is a curve in $\mathbb{R}^2$ which is, of course, one dimensional.

Next, define a map

$$\mathcal{F} : \mathbb{R}^2 \to \mathbb{R}^2, \quad \mathcal{F}\begin{bmatrix} \xi \\ \eta \end{bmatrix} = \begin{bmatrix} -\left(\frac{\rho_2}{\rho_1 + \rho_2}\xi + \frac{1}{\rho_1 + \rho_2}\eta\right) + GF_\nu\left(\frac{\rho_2}{\rho_1 + \rho_2}\xi + \frac{1}{\rho_1 + \rho_2}\eta\right) \\ \rho_2\left(\frac{\rho_2}{\rho_1 + \rho_2}\xi + \frac{1}{\rho_1 + \rho_2}\eta\right) + \rho_1 GF_\nu\left(\frac{\rho_2}{\rho_1 + \rho_2}\xi + \frac{1}{\rho_1 + \rho_2}\eta\right) \end{bmatrix}.$$

Then the iteration in (58) can be written as

$$(\xi_{n+1},\, \eta_{n+1}) = \mathcal{F}(\xi_n,\, \eta_n)\,, \quad n = 0,\, 1,\, 2, \ldots\,.$$

It is trivial to see that $\mathcal{F} : \mathbb{R}^2 \to \mathcal{C}$ and, therefore $\mathcal{F}$ has a restriction

$$\tilde{\mathcal{F}} \equiv \mathcal{F}|_{\mathcal{C}} : \mathcal{C} \to \mathcal{C}\,. \tag{59}$$

Let $\mathcal{G}$ be the graph of GF_ν:

$$\mathcal{G} \equiv \{(v,\, GF_\nu(v)) \in \mathbb{R}^2 | v \in \mathbb{R}\}\,.$$

Define

$$H : \mathcal{G} \to \mathcal{G}\,, \quad H \begin{bmatrix} v \\ GF_\nu(v) \end{bmatrix} = \begin{bmatrix} GF_\nu(v) \\ (GF_\nu)^2(v) \end{bmatrix}\,,$$

i.e. H is the diagonal operator

$$H = \begin{bmatrix} GF_\nu(\cdot) & 0 \\ 0 & GF_\nu(\cdot) \end{bmatrix}\,.$$

Let $Q : \mathbb{R}^2 \to \mathbb{R}^2$ be given by

$$Q \begin{bmatrix} \xi \\ \eta \end{bmatrix} = \begin{bmatrix} -\xi + \eta \\ \rho_2 \xi + \rho_1 \eta \end{bmatrix}\,.$$

Then Q is invertible and

$$\tilde{Q} \equiv Q|_{\mathcal{G}} : \mathcal{G} \to \mathcal{C} \quad \text{homeomorphically.}$$

Using the above, we easily verify that we have the commutative diagram

$$\begin{array}{ccc} \mathcal{G} & \xrightarrow{H} & \mathcal{G} \\ {\scriptstyle \tilde{Q}}\downarrow & & \downarrow{\scriptstyle \tilde{Q}} \\ \mathcal{C} & \xrightarrow{\tilde{\mathcal{F}}} & \mathcal{C} \end{array} \qquad \tilde{\mathcal{F}} = \tilde{Q} H \tilde{Q}^{-1} \tag{60}$$

Therefore $\tilde{\mathcal{F}}$ is topologically conjugate to a diagonal map H both of whose diagonal entries are the same map GF_ν, which is chaotic for ν and α, β lying in a certain parameter range. It is in the sense of topological conjugacy (59) that the gradient $(w_x(1,\, t),\, w_t(1,\, t))$ map (59), a Poincaré section of $(w_x(x,\, t),\, w_t(x,\, t))$ at $x = 1$, is chaotic.

Note that in general the state variable $w(x,\, t)$ *does not* display chaotic behavior. It only has a *fractal* outlook. In order to have chaotic profile of $w(x,\, t)$ itself, the boundary conditions must be differentiated. See the discussion in the next section.

5. Differentiability of Solutions

The smoothness of solutions to linear or nonlinear PDEs is always a major issue. Here, let us examine the questions of continuity and differentiability of the solutions u, v and consequently, w. We will follow [Chen *et al.*, 1998b, Sec. 6].

First, note from the explicit representations in (37) and (38) that u and v are obtained by patching up different expressions along the following characteristics:

$$\begin{cases} \rho_2 x + t = k(\rho_1 + \rho_2), \\ \rho_2 x + t = k(\rho_1 + \rho_2) + \rho_2, \\ \rho_1 x - t = -k(\rho_1 + \rho_2), \\ \rho_1 x - t = -k(\rho_1 + \rho_2) - \rho_2, \\ k = 0,\, 1,\, 2, \ldots,\, n, \ldots; \quad x \in [0,\, 1], \quad t \geq 0\,. \end{cases} \tag{61}$$

Only along these characteristics can discontinuities propagate [Courant & Hilbert, 1962, Sec. V.1]. Therefore, we need to study how smooth the patching in (37) and (38) is across the characteristic line segments in (61).

Theorem 5.1. *Let $(u,\, v)$ be the solution of the system (23), (26)–(28) in the sense of the method of characteristics as represented by (37) and (38). Assume that the initial conditions $u_0,\, v_0 \in C^m([0,\, 1])$ for some $m \in \{0,\, 1,\, 2, \ldots\}$. In addition, assume that at the left end $x = 0$, we have*

$$v_0^{(j)}(0) = (-1)^{j+1} \rho_1^{2j} u_0^{(j)}(0)\,, \quad j = 0,\, 1, \ldots,\, m\,. \tag{62}$$

Also at the right end $x = 1$, assume that we have

$$\begin{aligned} u_0^{(j)}(1) = (-1)^j \rho_2^{2j} \cdot \mathcal{F}_j(F_\nu,\, F_\nu',\, \ldots,\, F_\nu^{(j)},\, v_0(1), \\ v_0'(1), \ldots,\, v_0^{(j)}(1)), \quad j = 0,\, 1,\, 2, \ldots,\, m\,, \end{aligned} \tag{63}$$

where

$$\begin{aligned} &\mathcal{F}_0 = F_\nu(v_0(1)), \quad \mathcal{F}_1 = F_\nu'(v_0(1)) v_0'(1), \\ &\mathcal{F}_2 = F_\nu''(v_0(1)) v_0'(1)^2 + F_\nu'(v_0(1)) v_0''(1)\,, \\ &\mathcal{F}_3 = F_\nu'''(v_0(1))[v_0'(1)]^3 + 3F_\nu''(v_0(1)) v_0''(1) v_0'(1) \\ &\qquad + F_\nu'(v_0(1)) v_0'''(1)\,, \\ &\quad \vdots \\ &\mathcal{F}_m = F_\nu^{(m)}(v_0(1))[v_0'(1)]^m + \cdots + F_\nu'(v_0(1)) v_0^{(m)}(1). \end{aligned}$$

Then the solution $(u,\, v)$ is C^m-continuous on the space-time domain $\{(x,\, t) | 0 \leq x \leq 1,\, 0 \leq t \leq T\}$ for any $T > 0$.

Proof. Choose any unit vector $\mathbf{a} = (a_1, a_2)$ on the (x, t)-plane, and let $D_{\mathbf{a}}$ be the directional derivative along $\mathbf{a}$. We need to show that $(D_{\mathbf{a}})^j u$ and $(D_{\mathbf{a}})^j v$ are continuous across the characteristics line segments in (61), for any $k = 0, 1, 2, \ldots$, for $j = 0, 1, 2, \ldots, m$.

Take, for example, $(38)_1$ and $(38)_2$ across the characteristic segment $t - \rho_1 x = k(\rho_1 + \rho_2)$:

$$v(x, t) = \begin{cases} (G \circ F_\nu)^k(v_0(x - \rho_2\tau)) = (G \circ F_\nu)^k(v_0(x - \rho_2(t - k(\rho_1 + \rho_2)))), \\ \qquad t - k(\rho_1 + \rho_2) \le \rho_1 x \le \rho_1, \\ G \circ (F_\nu \circ G)^k(u_0(-\rho_1^2(x - \rho_2\tau))) = (G \circ F_\nu)^k(-u_0(-\rho_1^2 x + \rho_1(t - k(\rho_1 + \rho_2)))), \\ \qquad \rho_1 x < t - k(\rho_1 + \rho_2) \le \rho_1 x + \rho_2. \end{cases}$$

In order to have $v(x, t)$ C^m-continuous across $t - \rho_1 x = k(\rho_1 + \rho_2)$, we must have

$$D_{\mathbf{a}}^j[(G \circ F_\nu)^k(v_0(x - \rho_2 t + k\rho_2(\rho_1 + \rho_2)))] = D_{\mathbf{a}}^j[(G \circ F_\nu)^k(-u_0(-\rho_1^2 x + \rho_1 t - k\rho_1(\rho_1 + \rho_2)))]$$
$$\text{on } t - \rho_1 x = k(\rho_1 + \rho_2), \text{ for } k = 0, 1, 2, \ldots.$$

This leads to (62).

Similarly, we obtain (63) by the j-times differentiation $D_{\mathbf{a}}^j$ of $(37)_1$ and $(37)_2$ along the characteristic segments $t + \rho_2 x = \rho_2 + k(\rho_1 + \rho_2)$.

All the other cases in (37) and (38) lead to the same compatibility conditions (62) and (63). ■

Corollary 5.1. *Let w be the solution of (12) such that the initial conditions (w_0, w_1) satisfy $w_0 \in C^{m+1}([0, 1])$ and $w_1 \in C^m([0, 1])$ for some nonnegative integer m. Let (u_0, v_0) be defined as in (26) and assume that (u_0, v_0) satisfy (37) and (38). Then w is C^{m+1}-continuous on $[0, 1] \times [0, T]$ for any $T > 0$.*

Now, assume that the solution w of (12) is C^1-continuous. Take $\partial/\partial t$ of $(12)_1$–$(12)_3$. We see that $W(x, t) \equiv w_t(x, t)$ satisfies the following system

$$\begin{cases} W_{xx}(x, t) - \nu W_{xt}(x, t) - W_{tt}(x, t) = 0, & 0 < x < 1, \quad t > 0, \\ W_x(0, t) = 0, & t > 0, \\ W_x(1, t) = [\alpha - 3\beta W^2(1, t)]W_t(1, t), & t > 0, \\ W(x, 0) = w_1(x),\ W_t(x, 0) = w_0''(x) - \nu w_1'(x), & 0 < x < 1. \end{cases} \tag{64}$$

Note that the right end boundary condition $(64)_3$ is also a self-excitation boundary condition, analogous to the van der Pol ODE

$$\ddot{x} + (\alpha - 3\beta x^2)\dot{x} + \omega_0^2 x = 0.$$

The boundary condition $(64)_3$ involves W itself and thus causes significant complexity if the method of characteristics were to be applied to (64). Here, we bypass such a technical difficulty by regarding (64) as a differentiated solution of (12). For (64), chaotic behavior of the state variable or displacement $W(x, t)$ *itself* can be observed (while for (12) only the chaotic behavior of the *gradient* (w_x, w_t) may happen).

Theorem 5.2. *Let W be a C^m-continuous solution of (64) for some $m \ge 0$. Then W is unique. Assume that $\alpha, \beta, \nu > 0$ and $\alpha \le \rho_2(\nu)$ such that the map $G \circ F_\nu$ is chaotic. Then W displays chaotic behavior.*

Proof. The uniqueness of W follows from the fact that

$$w(x, t) \equiv \int_0^t W(x, \tau)d\tau + f_0(x), \quad 0 \le x \le 1,$$

where $f_0(x)$ is a C^{m+1}-continuous function satisfying $f_0'' = w_0''$ for w_0'' given in $(64)_4$ and appropriate compatibility conditions, is the unique solution of (12).

The reason that $W(x, t)$ can display chaotic behavior is that $W(x, t) = w_t(x, t)$ for w satisfying (12), and by Sec. 4, w_t displays chaotic behavior if the map $G \circ F_\nu$ is chaotic. ■

6. Numerical Examples

We offer numerical examples and graphics to manifest the difference in profiles between spatio-temporal-isotropic chaotic vibration in [Chen *et al.*, 1998b] and the nonisotropic chaotic vibration being studied here.

Example 6.1 (Isotropic Chaotic Vibration). Consider

$$\begin{cases} w_{xx}(x,\,t) - w_{tt}(x,\,t) = 0, & 0 < x < 1, \quad t > 0\,, \\ w_x(0,\,t) = -\eta w_t(0,\,t), & t > 0, \quad \eta > 0 \text{ is fixed}, \\ w_x(1,\,t) = \alpha w_t(1,\,t) - \beta w_t^3(1,\,t), & t > 0, \quad 0 < \alpha \le 1, \quad \beta > 0, \\ w(x,\,0) = w_0(x),\ w_t(x,\,0) = w_1(x), & 0 < x < 1\,. \end{cases} \tag{65}$$

Define

$$u(x,\,t) = \frac{1}{2}[w_x(x,\,t) + w_t(x,\,t)]\,,$$

$$v(x,\,t) = \frac{1}{2}[w_x(x,\,t) - w_t(x,\,t)]\,.$$

Then

$$u(x,\,0) = \frac{1}{2}[w_0'(x) + w_1(x)] \equiv u_0(x)\,,$$

$$v(x,\,0) = \frac{1}{2}[w_0'(x) - w_t(x)] \equiv v_0(x)\,.$$

Define the map

$$G(v) \equiv G_\eta(v) = -\frac{1+\eta}{1-\eta}v\,,$$

then $u(x,\,t)$ and $v(x,\,t)$ satisfy (37) and (38), with $\nu = 0$, $\rho_1(0) = \rho_2(0) = 1$, $G \equiv G_\eta$ and $F_\nu \equiv F_\nu|_{\nu=0} = F_0$. According to [Chen *et al.*, 1998b, Example 4.3], the map $G_\eta \circ F_0$ is chaotic when $\alpha = 0.5$, $\beta = 1$, $\eta = 1.520$, for example. Therefore both u and v display chaotic behavior. By choosing a C^2-spline

$$u_0(x) = \frac{1}{12}\begin{cases} \dfrac{(x-x_1)^3}{h^3}, & x_1 \le x \le x_2, \\ 1 + \dfrac{3(x-x_2)}{h} + \dfrac{3(x-x_2)^2}{h^2} - \dfrac{3(x-x_2)^3}{h^3}, & x_2 \le x \le x_3, \\ 1 - \dfrac{3(x-x_4)}{h} + \dfrac{3(x-x_4)^3}{h^2} + \dfrac{3(x-x_4)^3}{h^3}, & x_3 \le x \le x_4, \\ \dfrac{(x_5-x)^3}{h^3}, & x_4 \le x \le x_5, \\ 0, & \text{elsewhere}\,, \end{cases} \tag{66}$$

$$h = \frac{1}{6},\ x_j = \frac{j}{6}, \quad j = 1,\,2,\,3,\,4,\,5\,,$$

$$v_0(x) \equiv 0\,, \tag{67}$$

we have $u,\,v \in C^2([0,\,1] \times [0,\,T])$ for any $T > 0$.

The solution profiles of u and v are plotted in Figs. 8 and 9, respectively, for $t : 50 \cdot 2 \le t \le 51 \cdot 2$. (Note that here, each *cycle of vibration* which is the time required for a wave to travel from one end point and return, is two time units.) Even though there is chaotic vibration, there is clearly visible *orderly* patterns of wave propagation on the wave fronts $x + t = \text{const.}$ and $x - t = \text{const.}$ for u and v, respectively.

Example 6.2 (Nonisotropic Chaotic Vibration). Consider now (12) instead, with $\alpha = 0.5$, $\beta = 1$ and $\nu = 3.33$. Then

$$\rho_1(\nu) = 0.277\,, \quad \rho_2(\nu) = 3.61\,.$$

Each cycle of vibration takes $\rho_1 + \rho_2 \approx 3.88$ time units. According to Theorem 3.2, for these parameter values, the map $G \circ F_\nu$ is chaotic.

Choosing the same initial conditions for u_0 and v_0 as in (66) and (67), we note that Theorem 5.1

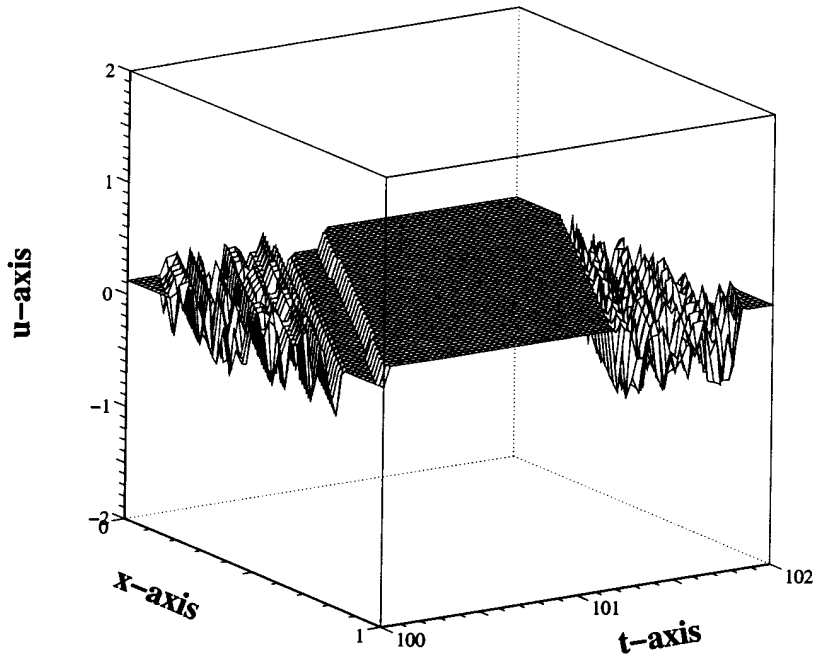

Fig. 8. The spatiotemporal–isotropic chaotic profile of $u(x, t)$, $0 \le x \le 1$, $50 \cdot 2 \le t \le 51 \cdot 2$, for Example 6.1. Note that chaotic wave fronts propagate with $x + t =$ constant.

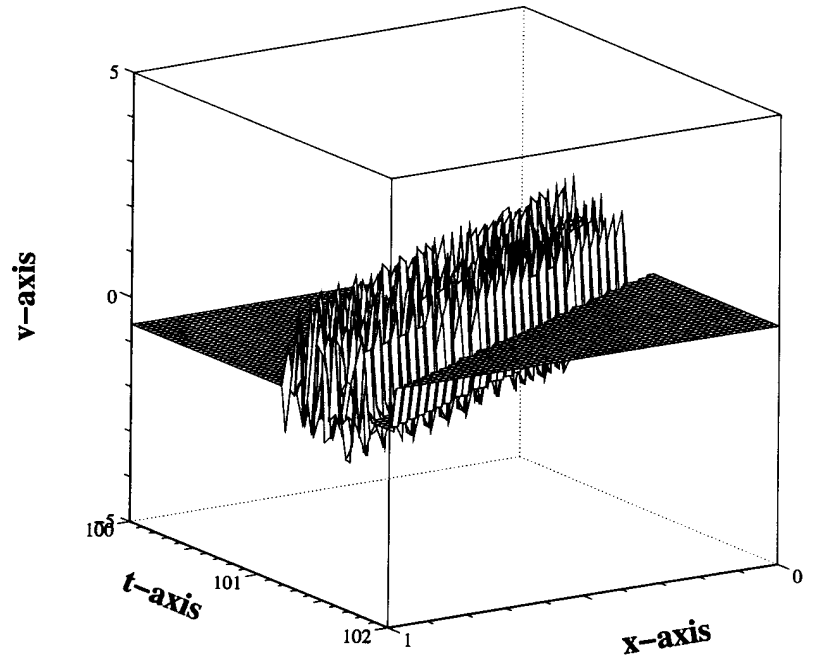

Fig. 9. The spatiotemporal–isotropic chaotic profile of $v(x, t)$, $0 \le x \le 1$, $50 \cdot 2 \le t \le 51 \cdot 2$, for Example 6.1. Note that chaotic wave fronts propagate with $x - t =$ constant.

is applicable, and we again have u, $v \in C^2([0, 1] \times [0, T])$, for any $T > 0$.

The solution profiles of u and v are plotted in Figs. 10–15, for $t : 0 \le t \le 3.88$, $3.88 \le t \le 2 \cdot 3.88$, and $50 \cdot (3.88) \le t \le 51 \cdot (3.88)$. The reader may observe sharp "randomness" in every direction of space and time. Thus, nonisotropic chaotic vibration shows strong mixing of waves.

The profiles of the gradient, w_t and w_x, are plotted in Figs. 16 and 17, respectively, for

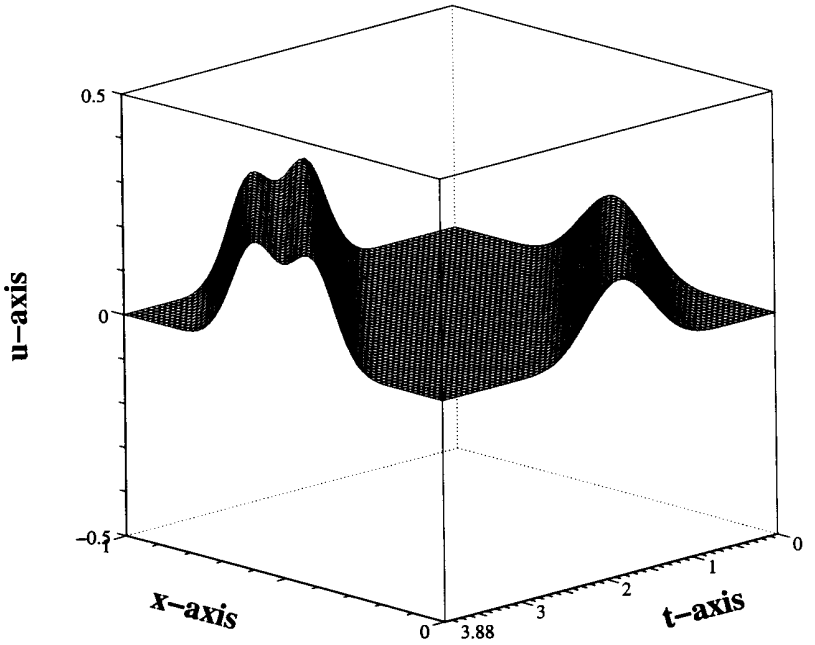

Fig. 10. The initial spatiotemporal profile of $u(x, t)$, $0 \le x \le 1$, $0 \le t \le 3.88$, for Example 6.2.

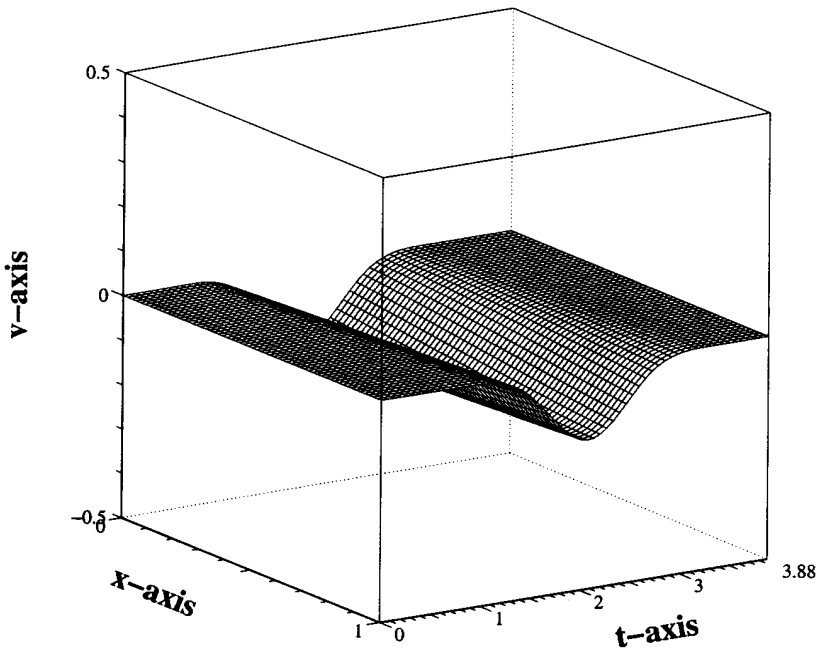

Fig. 11. The initial spatiotemporal profile of $v(x, t)$, $0 \le x \le 1$, $0 \le t \le 3.88$, for Example 6.2.

$50 \cdot (3.88) \le t \le 51 \cdot (3.88)$, according to (24). The profile of w itself is given in Fig. 14, with initial condition

$$w_0(x) = \int_0^x u_0(\xi) d\xi \,,$$

$$0 \le x \le 1; \text{ see (66) for } u_0 \,.$$

The reader may note the *fractal, but nonchaotic*, pattern of w.

7. Comments on Other Types of Boundary Conditions at $x = 0$

Heretofore, the boundary condition at $x = 0$ was

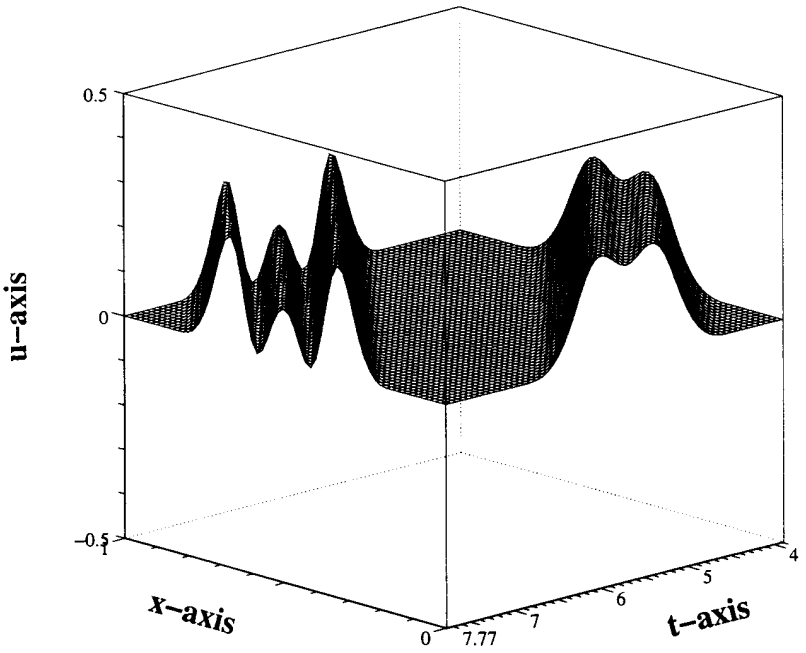

Fig. 12. The spatiotemporal profile of $u(x, t)$ during the second time-cycle, $0 \leq x \leq 1$, $3.88 \leq t \leq 2 \cdot (3.88)$, for Example 6.2.

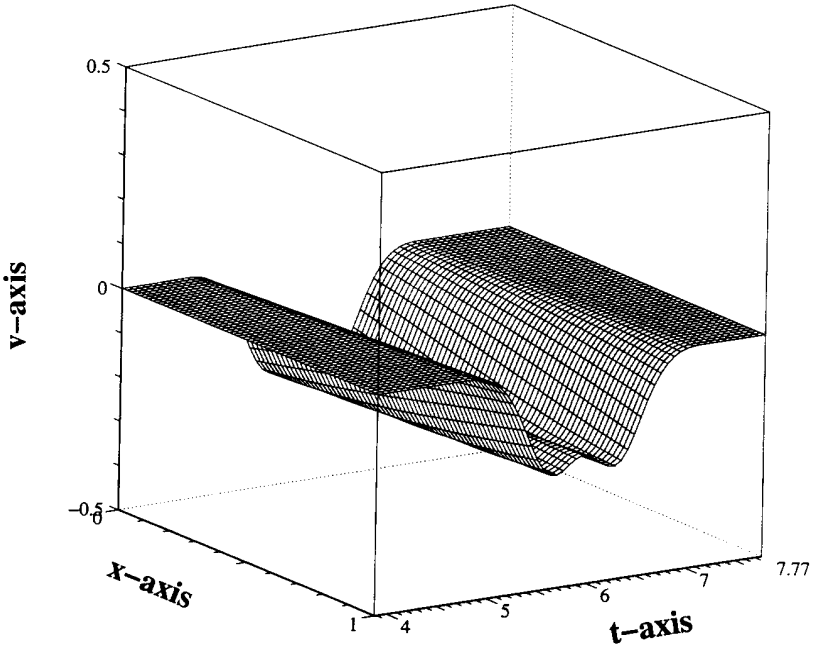

Fig. 13. The spatiotemporal profile of $v(x, t)$ during the second time-cycle, $0 \leq x \leq 1$, $3.88 \leq t \leq 2 \cdot (3.88)$, for Example 6.2.

assumed to be homogeneous Neumann as in $(12)_2$. But some other types of boundary conditions can be treated as well.

First, let us consider the Dirichlet boundary condition

$$w(0, t) = 0\,, \quad t > 0\,, \tag{68}$$

in lieu of $(12)_2$. The above gives

$$w_t(0, t) = 0\,,$$
$$\rho_1(\nu)u(0, t) - \rho_2(\nu)v(0, t) = 0\,, \quad \text{(by } (24)_2\text{)}$$

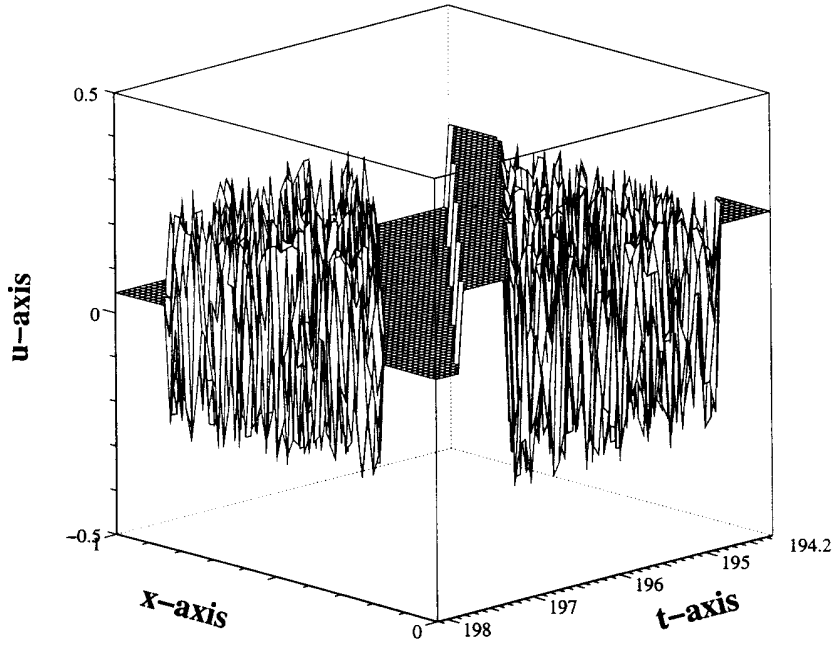

Fig. 14. The spatiotemporal–nonisotropic chaotic profile of $u(x, t)$, $0 \le x \le 1$, $50 \cdot (3.88) \le t \le 51 \cdot (3.88)$, for Example 6.2. Note the sharp 2D randomness in the chaotic zone.

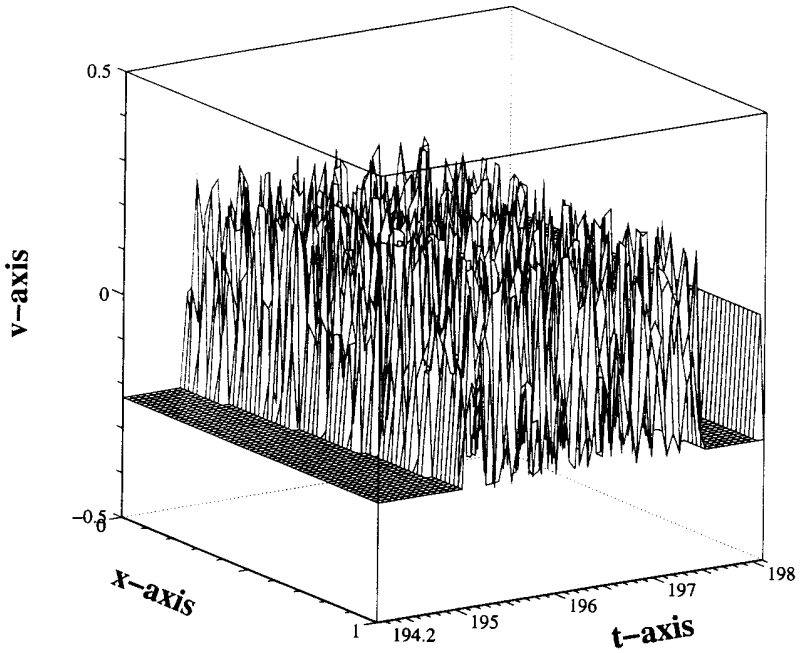

Fig. 15. The spatiotemporal–nonisotropic chaotic profile of $v(x, t)$, $0 \le x \le 1$, $50 \cdot (3.88) \le t \le 51 \cdot (3.88)$, for Example 6.2. Note the sharp 2D randomness in the chaotic zone.

and so the reflection relation at $x = 0$ is

$$v(0, t) = \frac{\rho_1(\nu)}{\rho_2(\nu)} u(0, t) \equiv G_\nu(u(0, t)) . \qquad (69)$$

The explicit representations (37) and (38) are again applicable, wherein G_ν in (69) is now replacing G in (27). Therefore, whether (the new) u and v display chaotic behavior depends on the orderly or chaotic property of the map $G_\nu \circ F_\nu$ and/or $F_\nu \circ G_\nu$. But $F_\nu \circ G_\nu$ is topologically conjugate to $F_\nu \circ G_\nu$ through the topological conjugacy

$$(G_\nu \circ F_\nu) \circ G_\nu = G_\nu \circ (F_\nu \circ G_\nu) ,$$

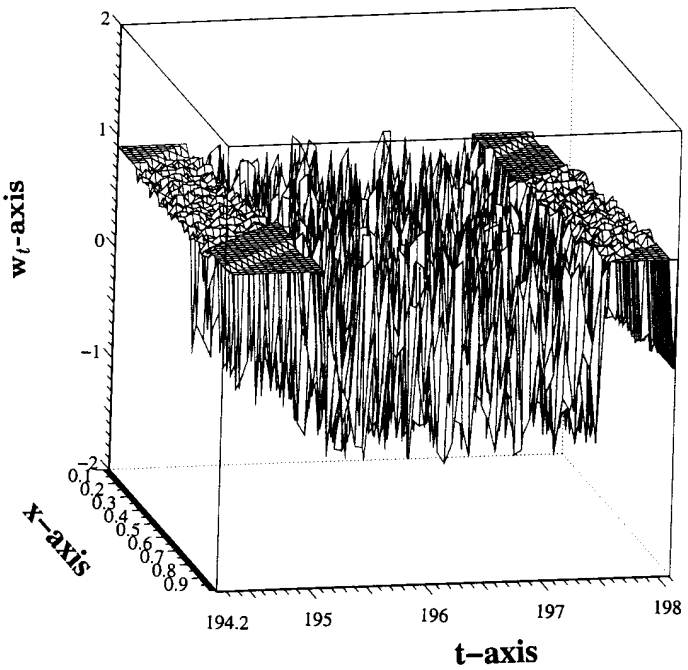

Fig. 16. The profile of $w_t(x, t)$, $0 \le x \le 1$, $50 \cdot (3.88) \le t \le 51 \cdot (3.88)$, for Example 6.2. Again note the spatiotemporal–nonisotropic chaotic feature as well as the mixture of very chaotic, mildly chaotic, and nonchaotic zones here and in Fig. 17 next.

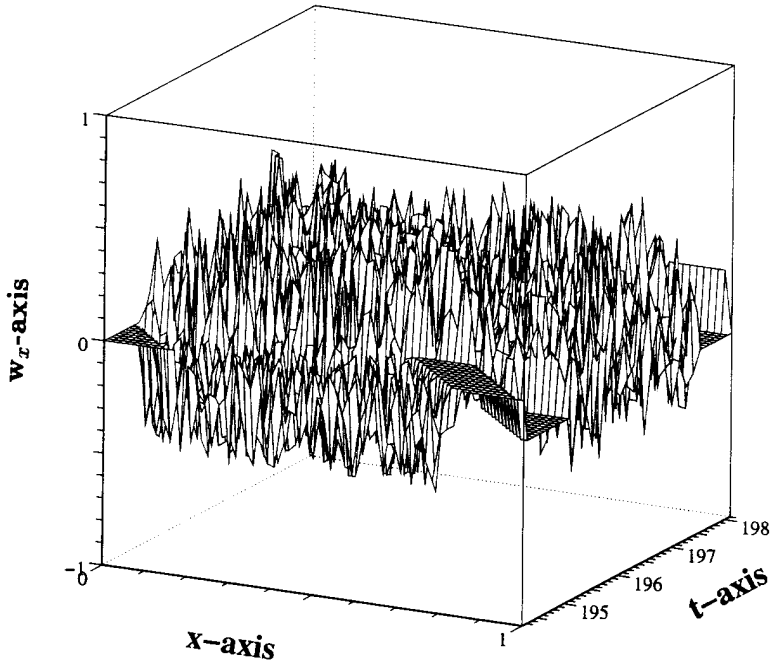

Fig. 17. The profile of $w_x(x, t)$, $0 \le x \le 1$, $50 \cdot (3.88) \le t \le 51 \cdot (3.88)$, for Example 6.2.

therefore investigation of $G_\nu \circ F_\nu$ alone suffices. Instead of repeating all the analysis work in Secs. 2–5, we simply point out the consequence: $G_\nu \circ F_\nu$ is *not chaotic*. The reason is that the map G_ν in (69) is very *strongly contracting* because by Remark 1.5, $\rho_1(\nu)/\rho_2(\nu)$ is considerably smaller than 1 in general. Therefore, we see that the postivity of T_1 in Remark 1.3(i) due to the Neumann boundary condition is very important. For the Dirichlet condition (68), $T_1 \equiv 0$ in (14); there is much less energy

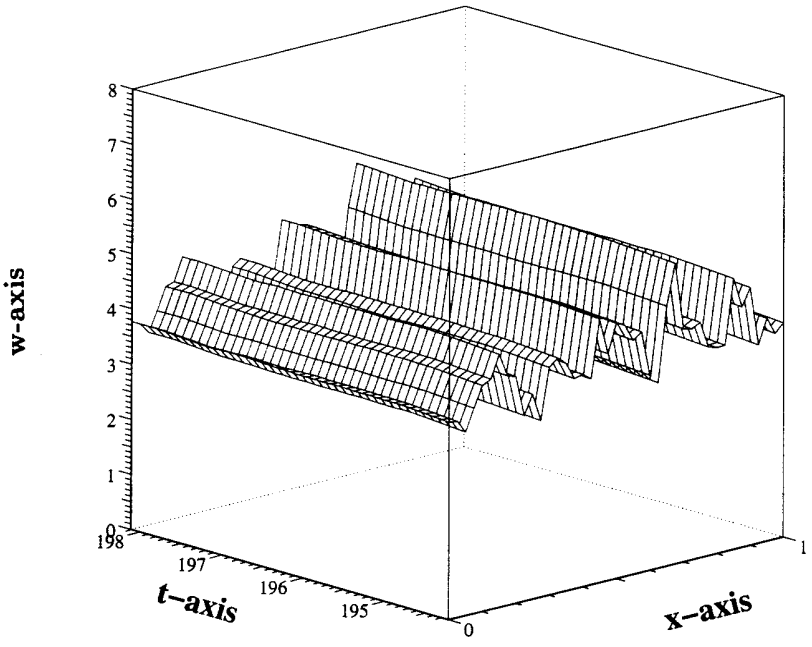

Fig. 18. The profile of the state variable $w(x, t)$, $0 \le x \le 1$, $50 \cdot (3.88) \le t \le 51 \cdot (3.88)$, for Example 6.2. Observe the fractal, but nonchaotic, appearance of w.

imbalance, which thus actually fails to produce chaos.

Second, if the boundary condition at $x = 0$ is energy-injecting:

$$w_x(0, t) = -\eta w_t(0, t)\,, \quad \eta > 0,\ \eta \neq \rho_1(\nu)\,, \quad (70)$$

in lieu of $(12)_2$, then the new reflection relation at $x = 0$ is

$$\begin{aligned} v(0, t) &= -\frac{1 + \rho_1(\nu)\eta}{1 - \rho_2(\nu)\eta} u(0, t) \\ &\equiv G_{\nu,\eta}(u(0, t))\,. \end{aligned} \quad (71)$$

One can use this $G_{\nu,\eta}$ instead of G in (27) to analyze the behavior of $G_{\nu,\eta} \circ F_\nu$. Again, as the parameter(s) η and/or ν vary, we observe chaos. However, (70) may actually be regarded as a "special case" as our treatment in Secs. 2–5, where we have shown that chaos occurs with $\eta = 0$ in (70), cf. $(12)_2$, i.e. we do not need extra energy injection like (70) at $x = 0$.

If the boundary condition at $x = 0$ is homogeneous Robin:

$$w(0, t) + \eta w_x(0, t) = 0\,, \quad \eta > 0, \quad \text{for all } t > 0\,,$$

then the treatment becomes much more difficult. No analytical results are available so far.

References

Chen, G., Hsu, S. B. & Zhou, J. [1998a] "Chaotic vibrations of the one-dimensional wave equation due to a self-excitation boundary condition, Part I, controlled hysteresis," *Trans. Amer. Math. Soc.* **350**, 4265–4311.

Chen, G., Hsu, S. B. & Zhou, J. [1998b] "Ibid, Part II, energy injection, period doubling and homoclinic orbits," *Int. J. Bifurcation and Chaos* **8**, 423–445.

Chen, G., Hsu, S. B. & Zhou, J. [1998c] "Ibid, Part III, natural hysteresis memory effects," *Int. J. Bifurcation and Chaos* **8**, 447–470.

Chen, G., Hsu, S. B. & Zhou, J. [1998d] "Snapback repellers as a cause of chaotic vibration of the wave equation with a van der Pol boundary condition and energy injection at the middle of the span," *J. Math. Phys.* **39**, 6459–6489.

Collet, C. & Tresser, C. [1978] "Itération d'endomorphismes et de groupe de renormalisation," *J. de Physique Colloque* **39**, C5–C25.

Courant, R. & Hilbert, D. [1962] *Methods of Mathematical Physics*, Vol. II (Wiley-Interscience, NY).

Devaney, R. L. [1989] *An Introduction to Chaotic Dynamical Systems* (Addison-Wesley, NY).

Feigenbaum, M. [1978] "Quantitative universality for a class of non-linear transformations," *J. Stat. Phys.* **21**, 25–52.

Herzel, H. [1993] "Bifurcation and chaos in voice signals," *Appl. Mech. Rev.* **46**, 399–413.

Holzfuss, J. & Lauterborn, W. [1989] "Liapunoff exponent from a time series of acoustic chaos," *Phys. Rev.* **A39**, 2146–2152.

Idogawa, T., Kobata, T., Komuro, K. & Iwaki, M. [1993] "Nonlinear vibrations in the air column of a clarinet artificially blown," *J. Acoust. Soc. Am.* **93**, 540–551.

Katz, R. A. [1996] *Chaotic Fractal and Nonlinear Signal Processing*, *AIP Conf. Proc.*, Vol. 375 (Am. Inst. Phys., Woodbury, NY).

Lauterborn, W. & Cramer, E. [1981] "Subharmonic route to chaos observed in acoustics," *Phys. Rev. Lett.* **47**, 1445–1448.

Lauterborn, W. & Holzfuss, J. [1986] "Evidence for a low-dimensional strange attractor in acoustic turbulence," *Phys. Lett.* **A115**, 369–372.

Lauterborn, W., Parlitz, U., Holzfuss, J., Billo, A. & Akhatov, I. [1996] "Acoustic chaos," in *Chaotic, Fractal and Nonlinear Signal Processing*, ed. Katz, R. A. (AIP Press, Woodbury, NY), pp. 217–230.

Mcintyre, M. E., Schumacher, R. T. & Woodhouse, J. [1983] "On the oscillations of musical instruments," *J. Acoust. Soc. Am.* **74**, 1325–1345.

Mende, W., Herzel, H. & Wermke, K. [1990] "Bifurcation and chaos in newborn infant cries," *Phys. Lett.* **A145**, 418–424.

Robinson, C. [1995] *Dynamical Systems, Stability, Symbolic Dynamics and Chaos* (CRC Press, Boca Raton, FL).

Sharkovsky, A. N., Maistrenko, Y. L. & Romanenko, E. Y. [1993] *Difference Equations and Their Applications* (Kluwer, Dordrecht, The Netherlands).

Sharkovsky, A. N. [1994] "Ideal turbulences in an idealized time-delayed Chua's circuit," *Int. J. Bifurcation and Chaos* **4**, 303–309.

Shigesada, N., Kawasaki, K. & Teramoto, E. [1979] "Spatial segregation of interacting species," *J. Theoret. Biol.* **79**, 83–99.

Shimura, M. [1967] "Analysis of some nonlinear phenomena in a transmission line," *IEEE Trans. Circuit Th.* **14**, 60–69.

Smith, C. W., Tejwani, M. J. & Farris, D. A. [1982] "Bifurcation universality for first-sound subharmonic generation in superfluid helium," *Phys. Rev. Lett.* **48**, 492–494.

Stinecke, I. & Herzel, H. [1995] "Bifurcations in an asymmetric vocal-fold model," *J. Acoust. Soc. Am.* **97**, 1874–1884.

Stoker, J. J. [1950] *Nonlinear Vibrations* (Wiley-Interscience, NY).

Swift, G. W. [1988] "Thermoacoustic engines," *J. Acoust. Soc. Am.* **84**, 1145–1180.

Swift, G. W. [1995] "Thermoacoustic engines and refrigerators," *Phys. Today* **48**, 22–28.

Tufilaro, N. B. [1989] "Nonlinear and chaotic string vibrations," *Am. J. Phys.* **57**, 408–414.

Yazaki, T. [1993] "Experimental observation of thermoacoustic turbulence and universal properties at the quasiperiodic transition to chaos," *Phys. Rev.* **E48**, 1806–1818.